IBRO Neuroscience Reports 16 (2024) 224–240

Contents lists available at ScienceDirect

IBRO Neuroscience Reports

journal homepage: www.sciencedirect.com/journal/IBRO-Neuroscience-Reports

Research paper

Dose-dependent changes in orientation amplitude maps in the cat visual cortex after propofol bolus injections

Svetlana I. Shumikhina [a,*], Sergei A. Kozhukhov [b], Igor V. Bondar [b]

[a] Functional Neurocytology, Institute of Higher Nervous Activity and Neurophysiology, Russian Academy of Sciences, 5a Butlerova Street, 117485 Moscow, Russian Federation

[b] Physiology of Sensory Systems, Institute of Higher Nervous Activity and Neurophysiology, Russian Academy of Sciences, 5a Butlerova Street, 117485 Moscow, Russian Federation

ARTICLE INFO

Keywords:
Intrinsic optical imaging
Orientation selectivity
Plasticity
Anesthesia
Propofol

ABSTRACT

A general intravenous anesthetic propofol (2,6-diisopropylphenol) is widely used in clinical, veterinary practice and animal experiments. It activates gamma- aminobutyric acid (GABAa) receptors. Though the cerebral cortex is one of the major targets of propofol action, no study of dose dependency of propofol action on cat visual cortex was performed yet. Also, no such investigation was done until now using intrinsic signal optical imaging. Here, we report for the first time on the dependency of optical signal in the visual cortex (area 17/area 18) on the propofol dose. Optical imaging of intrinsic responses to visual stimuli was performed in cats before and after propofol bolus injections at different doses on the background of continuous propofol infusion. Orientation amplitude maps were recorded. We found that amplitude of optical signal significantly decreased after a bolus dose of propofol. The effect was dose- and time-dependent producing stronger suppression of optical signal under the highest bolus propofol doses and short time interval after injection. In each hemisphere, amplitude at cardinal and oblique orientations decreased almost equally. However, surprisingly, amplitude at cardinal orientations in the ipsilateral hemisphere was depressed stronger than in contralateral cortex at most time intervals. As the magnitude of optical signal represents the strength of orientation tuned component, these our data give new insights on the mechanisms of generation of orientation selectivity. Our results also provide new data toward understanding brain dynamics under anesthesia and suggest a recommendation for conducting intrinsic signal optical imaging experiments on cortical functioning under propofol anesthesia.

1. Introduction

Propofol (2,6-diisopropylphenol) is a general anesthetic which is often used in clinical (Langley and Heel, 1988; Marik, 2004; Dunn et al., 2007; Ota et al., 2010; Li et al., 2013) and veterinary practice (Morgan and Legge, 1989; Glowaski and Wetmore, 1999; Short and Bufalari, 1999; Sano et al., 2003; Monteiro et al., 2014), and animal experiments (Brown et al., 2003; Samonds and Bonds, 2005). After intravenous injection, propofol rapidly exerts its anesthetic effect (Major et al., 1981; Langley and Heel, 1988). Short recovery time after single injections allows using it for small surgical procedures (Glowaski and Wetmore, 1999; Langley and Heel, 1988; Dunn et al., 2007). Propofol can also be used for long-lasting surgeries and experiments by maintaining its blood concentration with a continuous infusion, or by single bolus injections (Langley and Heel, 1988; Cavazzuti et al., 1991; Raszplewicz et al., 2013).

Propofol exerts its anesthetic effect mainly by facilitating intracortical inhibition via activation of benzodiazepine gamma- aminobutyric acid (GABAa) receptors (ligand-gated Cl^- channels) (Collins, 1988; Concas et al., 1990; Fritschy and Panzanelli, 2014; Hao et al., 2020; Kobayashi and Oi, 2017). It also modulates ion channels that determine firing properties of neurons. It inhibits voltage-gated Na^+ currents (INa) that are important for the generation and propagation of action potentials (Ratnakumari and Hemmings, 1997; Rehberg and

Abbreviations: CB, cardinal bias; EEG, electroencephalogram; GABA, gamma- aminobutyric acid; Ih, a hyperpolarization-activated pacemaker inward current; Ik, the delayed rectifier potassium current; INa, voltage-gated Na+ currents; K-W ANOVA test, Kruskal-Wallis One-Way ANOVA test; N-K test, nonparametric Newman–Keuls' Multiple Comparisons test; ROI, region of interest; t-test, two-tailed t-test; U test, Wilcoxon Rank Sum/Mann-Whitney U test.

* Corresponding author.
E-mail addresses: shumikhs3@yahoo.com (S.I. Shumikhina), bondar_iv@inbox.ru (I.V. Bondar).

https://doi.org/10.1016/j.ibneur.2023.12.010
Received 21 August 2023; Accepted 30 December 2023
Available online 10 January 2024

Duch, 1999; Ouyang et al., 2003; Martella et al., 2005). Potassium channels are also important regulators of neuronal excitability. They set the resting membrane potential and firing thresholds, repolarize action potentials, and limit excitability (Debanne et al., 2011). They determine the shape and the rate of action potentials (Jensen et al., 2011). Propofol inhibits the delayed rectifier potassium current (Ik) slowing the recovery of Ik from inactivation (Song et al., 2011; Zhang et al., 2016). Propofol inhibits K^+-evoked glutamate release mediated by activation of GABAa receptors (Buggy et al., 2000) and Na+ channel-mediated glutamate release (Lingamaneni et al., 2001). Propofol also suppresses a hyperpolarization-activated pacemaker inward current (Ih) (Funahashi et al., 2001; Chen et al., 2005; Ying et al., 2006) that could result in a decline of neuronal activity. Propofol suppresses voltage-gated Ca2 + currents which regulate firing properties of neurons such as spike-timing, burst-firing, and action potential threshold (Inoue et al., 1999; Martella et al., 2005; Debanne et al., 2011; Liu et al., 2019). Thus, propofol depresses brain activity by increasing inhibition and diminishing excitation. The *in vitro* experiments (Collins, 1988; Concas et al., 1990; Ratnakumari and Hemmings, 1997; Inoue et al., 1999; Rehberg and Duch, 1999; Funahashi et al., 2001; Ouyang et al., 2003; Chen et al., 2005; Martella et al., 2005; Ying et al., 2006; Lingamaneni et al., 2001; Song et al., 2011; Zhang et al., 2016; Liu et al., 2019) showed that propofol is acting in a concentration-dependent manner.

The cerebral cortex is one of the major targets of propofol action (Liu et al., 2013). However, there is a lack of *in vivo* investigations of dose dependency of propofol action on cortical activity. The *in vivo* investigations were mostly performed on the somatosensory cortex of the rat (Tan et al., 1993; Logginidou et al., 2003; Reed and Plourde, 2015) and primate (Ishizawa et al., 2016) and auditory cortex of the rat (Antunes et al., 2003) and human (Dueck et al., 2005). It was reported that the propofol effect can differ between different cortical areas (Ishizawa et al., 2016). However, there is a shortage of *in vivo* data on the dose dependency of propofol action in visual cortex. It is shown only, in rat primary visual cortex, that propofol injection changes the resting-state fMRI functional connectivity in the dose-dependent manner (Liu et al., 2013). Another fMRI study in rat primary visual cortex showed that propofol greatly decreases the dynamic repertoire of brain states (Hudetz et al., 2015). Propofol diminishes visual cortical evoked potential amplitude in rats, reducing both the ON and OFF components and spontaneous activity (Arena et al., 2017). No study of dose dependency of propofol action on cat visual cortex was performed yet. Also, no such investigation was done until now using intrinsic signal optical imaging.

Intrinsic signal optical imaging allows visualizing the neuronal activity from a large population of cortical neurons with a high spatial resolution (~50 μm) (for review, see Zepeda et al., 2004). The optical imaging technique was developed by Grinvald with coauthors (Grinvald et al., 1986; Frostig et al., 1990; Ts'o et al., 1990). This technique is based on the registration of optical properties of the nervous tissue that result from the increased oxygen consumption by active neurons (Frostig et al., 1990; Vanzetta and Grinvald, 1999). The neuronal activation leads to changes in the light scattering. The process is biphasic, with a local increase in deoxy-hemoglobin concentration following by an increase in oxy-hemoglobin corresponding to an initial decrease and later increase in reflected light intensity (Zhao et al., 2007). Intrinsic optical signals reflects both spiking and subthreshold activity (Das and Gilbert, 1995; Toth et al., 1996). The optical imaging technique allowed to visualize in details functional maps for orientation, direction, spatial frequency and ocular dominance in the visual cortex. Visual cortex has a columnar organization where cells in each column from superficial to deep layers prefer the same orientation of the visual stimulus as was first established in electrophysiological experiments in cats (Hubel and Wiesel, 1962) and confirmed in optical imaging experiments in cats (Grinvald et al., 1986; Bonhoeffer and Grinvald, 1991; Hübener et al., 1997) and monkeys (Ts'o et al., 1990; Grinvald et al., 1991).

Orientation selectivity is a distinctive feature of visual cortical neurons. It is established at the cortical level owing to the convergent afferent geniculocortical projections and local cortical circuits (Vidyasagar and Eysel, 2015). Many studies have demonstrated the importance of inhibition in generating and shaping orientation selectivity (for review, see Vidyasagar et al., 1996; Ferster and Miller, 2000; Alitto and Dan, 2010; Priebe, 2016).

It was shown in animals and humans that more neurons in visual cortex respond to cardinal (vertical and horizontal) than to oblique orientations (the so-called "oblique effect") (Coppola et al., 1998; Yu and Shou, 2000; Dragoi et al., 2001; Kenet et al., 2003; Wang et al., 2003a, Wang et al., 2003b; Wang, 2004; Coppola and White, 2004; Liang et al., 2007; Shen et al., 2008). The effect is not equally observed in different species. The most controversial results were reported about overrepresentation of cardinal orientations in the cat visual cortex. Some authors report the overrepresentation of neurons responding to cardinal contours in cats (Yu and Shou, 2000; Dragoi et al., 2001; Li et al., 2003; Kenet et al., 2003; Wang et al., 2003a, Wang et al., 2003b; Wang, 2004) while other authors could not find clear differences between representation of cardinal and oblique orientations both in electrophysiological experiments (Hubel and Wiesel, 1962; Campbell et al., 1968; Rose and Blakemore, 1974) and in optical imaging studies (Bonhoeffer and Grinvald, 1993; Müller et al., 2000; Ribot et al., 2008). The mechanisms of the "oblique effect" are still not fully understood. However, it has been suggested that more circuitry in the visual cortex is devoted to processing contours oriented along cardinal axes than to oblique contours (Wang et al., 2003b). It was also noticed that responses evoked by cardinal stimuli were generally greater than those by oblique stimuli (Yu and Shou, 2000) though no details were provided.

Here, we investigated the dose-depended changes in orientation amplitude maps recorded with an intrinsic signal optical imaging method in the cat visual cortex after propofol bolus injections. As propofol depresses neuronal activity in the visual cortex, one may expect that different doses will produce different changes in orientation selectivity maps including specific changes in the strength of suppression at cardinal and oblique orientations. This may involve also connections between different cortical areas which can be differently affected by propofol. Our experiments showed that propofol decreases the amplitude of the optical signal in a dose-dependent manner. Amplitude at cardinal and oblique orientations decreased almost equally in each hemisphere. However, surprisingly, amplitude at cardinal orientations in the ipsilateral hemisphere was depressed stronger than in contralateral cortex at most time intervals.

2. Material and methods

2.1. Animals and surgical preparation

Experiments were performed on nine adult cats of either sex. The study was carried out in accordance with the European Communities Council Directive of 24 November 1986 (86/609/ EEC) revised 22 September 2010 (Directive 2010/63/EU of the European Parliament and of the Council). The experimental protocol was approved by the Ethical Commission of the Institute of Higher Nervous Activity and Neurophysiology of the Russian Academy of Sciences. All efforts were made to minimize the number of animals used and their suffering.

Surgical preparations included tracheotomy for artificial ventilation, forelimb vein cannulation, craniotomy (16 mm diameter) over the visual cortex (areas 17 and 18) of both hemispheres and durotomy that were done under anesthesia with ketamine hydrochloride (Calypsol, Gedeon Richter Plc., Budapest, Hungary; 10–15 mg/kg, i/m) in combination with vetranquil (Ceva Santé Animale, Libourne, France; 30–40 mg/kg). Propofol bolus was injected in the dose that allowed a tracheal intubation. Animals placed in the stereotaxic apparatus were paralyzed with arduan (Gedeon Richter Plc., Budapest, Hungary, 0.2–0.4 mg/kg, i/v) in 5% dextrose lactated Ringer's nutritive solution. Arduan (0.2–0.4 mg/kg) was also administered every 1.5–2 h for additional animal

relaxation. Anesthesia sustained with propofol (0.4%, Diprivan, Fresenius Kabi, Bad Homburg, Germany; i/v). Propofol was delivered continuously at 2–4 mg/kg/h**.** In addition, butomidor (Richter Pharma AG, Wels, Germany; SC 2–4 mg/kg) was administered every 6 h to reduce pain. The anti-inflammatory agent dexamethasone (Shreya Life Sciences Pvt. Ltd, Mumbai, India; 2–4 mg/kg) was also injected subcutaneously. Adequate level of anesthesia was controlled by observing CO_2 concentration in the expired air (3.8–4.0%), heart rate (120–160 beats/min), body temperature (38.5 °C) and EEG. The head of each animal was set in the stereotaxic apparatus with ear, mouth, and orbital bars. The orbital bar pressed lightly on the eyeball, restricting its movement. Pupils were dilated with atropine (1%) and the nictitating

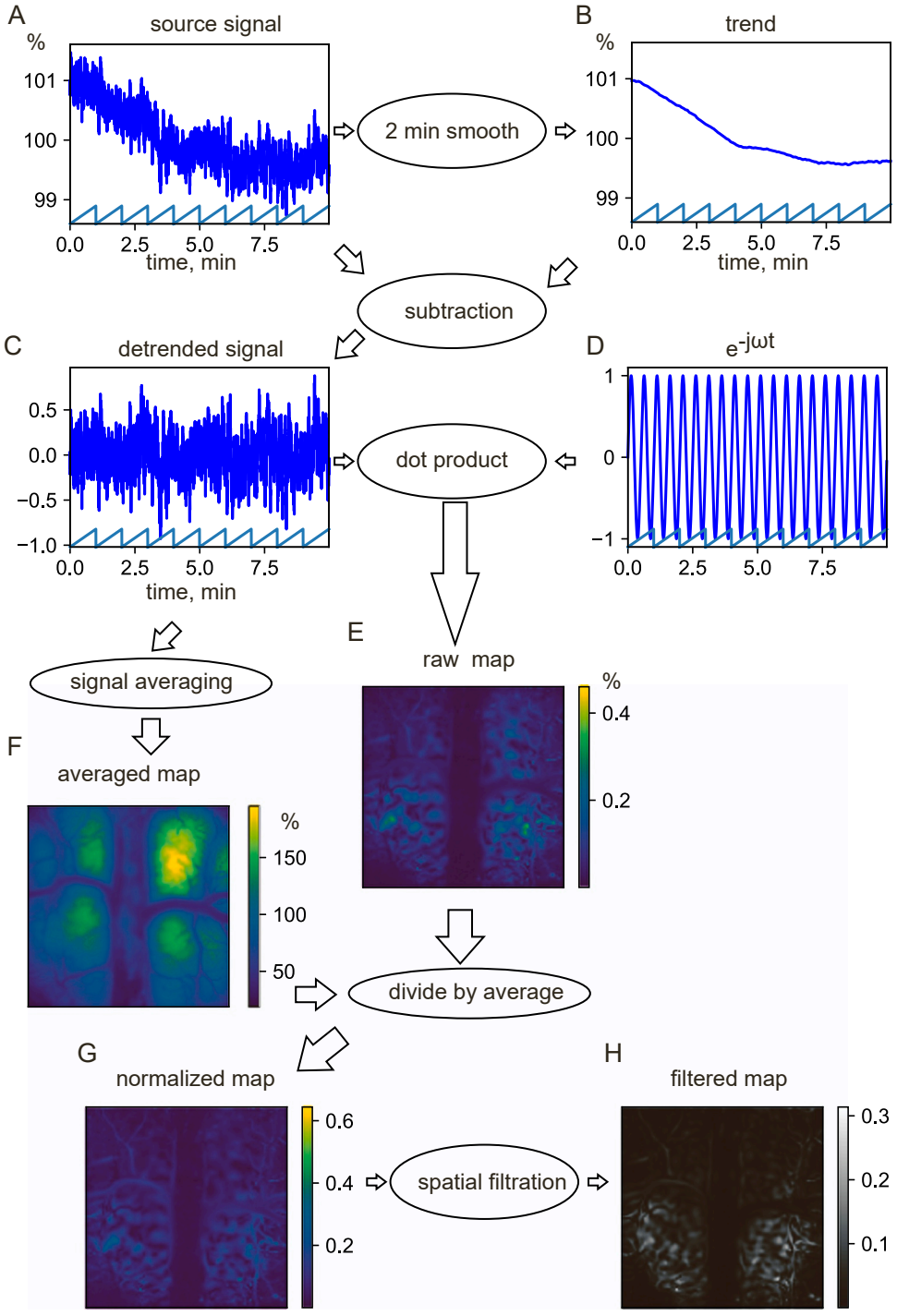

Fig. 1. Construction of orientation maps. A, time course of the light reflectance signal from a set of 4778 images (frames) of the visual cortex at one pixel. Y-axis: signal amplitude (dark blue) as the percentage of its average value for a given epoch of analysis (10 min). The synchronization signal is shown in light blue. B, the isoline (trend) of the response obtained after smoothing the signal by a sliding-window averaging over a window of one stimulus cycle (1 min). Same conventions as in A. C, the detrended signal after the isoline subtraction. D, the reference signal (sinusoid) at the double frequency of visual stimulation for a calculation of the second harmonic amplitude at one pixel. E, a raw map of the orientation amplitude (the scalar product of the signal after a subtraction of the isoline and reference signal). F, the averaged map with averaged values of the signal for a given epoch of analysis. G, the normalized map after dividing the raw map shown in E to the averaged value of the signal. H, the orientation amplitude map after high-pass and low-pass filtering.

membranes were contracted with phenylephrine hydrochloride ophthalmic solution (Iriphrine, Sentiss Pharma Private Limited, Haryana, India; 2.5%). Plano contact lenses were placed on the cat's eyes to protect the cornea from drying. One eye was closed with a non-transparent partition. Additionally, the eyelids were opened with a lid retractor, which also restricted eyeball movement.

After durotomy, the opening was covered with agarose (Fluka Biochemicals, Sigma Aldrich; 3%) with a low temperature of hardening. A cover glass was placed above the agarose.

2.2. Visual stimulation

Visual stimuli were generated by custom-made software developed by Dr. V.Kalatsky (ContStim, VK Imaging, Houston, Texas, USA) and displayed on a cathode ray screen (LG Flatron 795RT Plus, effective display area of 305 ×235 mm, mean luminance 40 cd/m^2, with a refresh rate of 70 Hz) placed 57 cm from the cat's eyes, centered on the representation of the area centralis and synchronized with the data acquisition processes. The requirements to parameters of a visual stimulus for continuous-periodic stimulation were described and fully explained by V.Kalatsky (2009). Monocular stimulation under scotopic (dark) adaptation was used. The stimulus was a moving clockwise full-screen drifting (a temporal frequency of 2 cycles/s) and rotating (angle speed of 1 rotation per minute, or 0.0167 Hz, 360° /min rotation) square-wave grating (100% contrast, a spatial frequency of 0.2 cycles/deg.). Note that since direction selectivity is not a factor, contours rotated through 180° are equivalent. The full-field grating can be moved only perpendicular to itself; translations parallel to the lines of the grating have no effect (Kalatsky, 2009). Orientations were changed continuously (i.e., without any interruption, according to the method of Kalatsky and Stryker (2003)). Each cycle of visual stimulation (60 s) included an infinite number of orientations with opposite stimulus directions. The grating orientation advanced by 22.5∘ every 3.75 s, such that a 180∘ cycle was completed every 30 s

2.3. Optical imaging

Intrinsic optical imaging was done using continuous-periodic visual stimulation with continuous data acquisition (method of Kalatsky and Stryker (2003)). A CCD camera (Dalsa 1M60P, USA) with 1024 × 1024 pixels in a matrix of 12 × 12 mm) was equipped with a tandem-lens macroscope (Ratzlaff and Grinvald., 1991; Grinvald et al., 1994). The surface vascular pattern was recorded with green illuminating light (546 nm). After acquisition of a surface image, the camera was focused 600–700 μm below the cortical surface. Intrinsic signals reflected from the cortical surface illuminated with 630 nm red light were recorded. The imaging system with data acquisition software developed by Dr. V. Kalatsky (VK Imaging, Houston, Texas, USA) acquired frames at the rate of 30 frames per second. Binning by 2 × 2 pixels spatially allowed storing frames as 512 × 512-pixel images.

Fig. 1 provides details of separation of the optical signal from the background signal (Fig. 1A). With a continuous-periodic stimulation with continuous acquisition paradigm, where Fourier transform is used to isolate the optical signal, the signal is extracted at the stimulation frequency (1 rotation per minute, or 0.0167 Hz in our case). The last one is chosen to stay safely from the low- and high-frequency bands of the physiological noise such as vasomotor signal (0.05–0.1 Hz), respiration rate (0.3–1 Hz), heart beat (2–5 Hz), and nonperiodic slow variation of the baseline due to the state of the subject (time scale is 1 min and up) (Kalatsky and Stryker, 2003). To remove the slow variation (Fig. 1B), the response was time averaged over a window of one stimulus cycle by the sliding-window analysis. Then the obtained trend was subtracted from the response (Fig. 1C). Fourier decomposition was performed on the detrended signal for each single pixel (Fig. 1D) to retrieve the amplitude and phase component of the signal. (The latter was used for construction of orientation preference maps, not demonstrated here but shown further in Figs. 2 and 3). The scalar product of the detrended signal on the reference signal (sinusoid) at the frequency equal to the double frequency of visual stimulation (the second harmonic) was computed. The obtained value corresponded to a neurons' selectivity for a given pixel. The values were joined for all pixels in the imaged area (dot product, in the complex plane). As a result, we obtained orientation selectivity (amplitude) maps (Fig. 1E). The orientation strength map was contaminated by two artifacts. The first artifact was related to unequal illumination of different cortical loci while the second one was due to the presence of very slow vasomotion waves. To remove the first artifact, all images (frames) were averaged and the averaged map was obtained (Fig. 1F). The raw map (Fig. 1E) was divided by the averaged map (Fig. 1F). As a result, the normalized map (Fig. 1G) was obtained where artifacts related to unequal illumination were removed. Finally, to remove artifacts related to vasomotion waves, we used the fact, that the very slow vasomotion waves correspond to spatial low frequency components while cortical functional modules correspond to high frequency components (Mayhew et. al., 1996), the images were low-pass and high-pass filtered in space (a low-frequency filter with a radius of 63 μm and a high-frequency filter with a radius of 630 μm). As a result, the orientation amplitude map was obtained (Fig. 1H) which was further analyzed. Response amplitudes in our experiments represent ΔR/R values (where R is light-reflected), similar to Craddoc et al. (2023).

Data were collected during one hour of continuous stimulation. As our previous experiments showed, maps recorded over a period of more than one hour could show some instability (Shumikhina et al., 2018). Thus, some processes occurring after one hour of stimulation could interfere with effects of the bolus propofol injection and hence were avoided by limiting the data collection period to 1 h only. In each cat, tests with one of the used bolus doses began in several hours after administration of propofol bolus for tracheal intubation, i.e., after completing surgical procedures and preliminary tests using optical imaging. A bolus dose of propofol (2, 3 or 4 mg/kg) was injected to the animal after control orientation maps were generated during 12 cycles of stimulation. Higher propofol bolus doses we did not use as a stronger suppression of cortical activity may not allow to record reliable maps.

2.4. Analysis of imaging data and statistics

Recordings accumulated during one hour were subdivided in 5 parts (epochs of analysis) each 12 min long. The signal was analyzed for a period of 10 min (cycles). The first and the 12th cycles for each period served for a construction of isoline to correct for border effects. The 10 min time period was taken to permit a precise estimation of the effects of propofol injections in time. It was shown that reliable orientation maps can be acquired with stimulation of 10 min or less using the approach of continuous stimulus presentation and data acquisition (Kalatsky and Stryker, 2003) which we used in the present study. The first part (Map-1, 0–12 min, referred as "0 min") was considered as a control. Four following parts (epochs of analysis) of one-hour continuous recording included recordings obtained after bolus propofol injection in 12 min (12 – 24 min, referred as "12 min"), 24 min (24–36 min, referred as "24 min"), 36 min (36–48 min, referred as "36 min"), and 48 min (48–60 min, referred as "48 min").

The map analysis was performed as described previously (Shumikhina et al., 2018). The analysis was done on a pixel-by-pixel basis in the region of interest (ROI). Tests were performed to localize areas 17 and 18. As was found in electrophysiological experiments, neurons in area 17 whose receptive fields are located within 5 degrees of the area centralis respond optimally to high spatial frequencies (0.2–3 cycles/deg, Movshon et al., 1978) while the optimal spatial frequency for cells in area 18 is between less than 0.1 and 0.5 cycles/deg (Movshon et al., 1978). In optical imaging experiments, the values of preferred spatial frequencies were reported in the range of 0.274 to 1.937 cycles/deg for area 17 (Ribot et al., 2013, the median 0.53 cycles/deg (Issa et al., 2000)) and < 0.274 cycles/deg for area 18 (Ribot et al., 2013, the

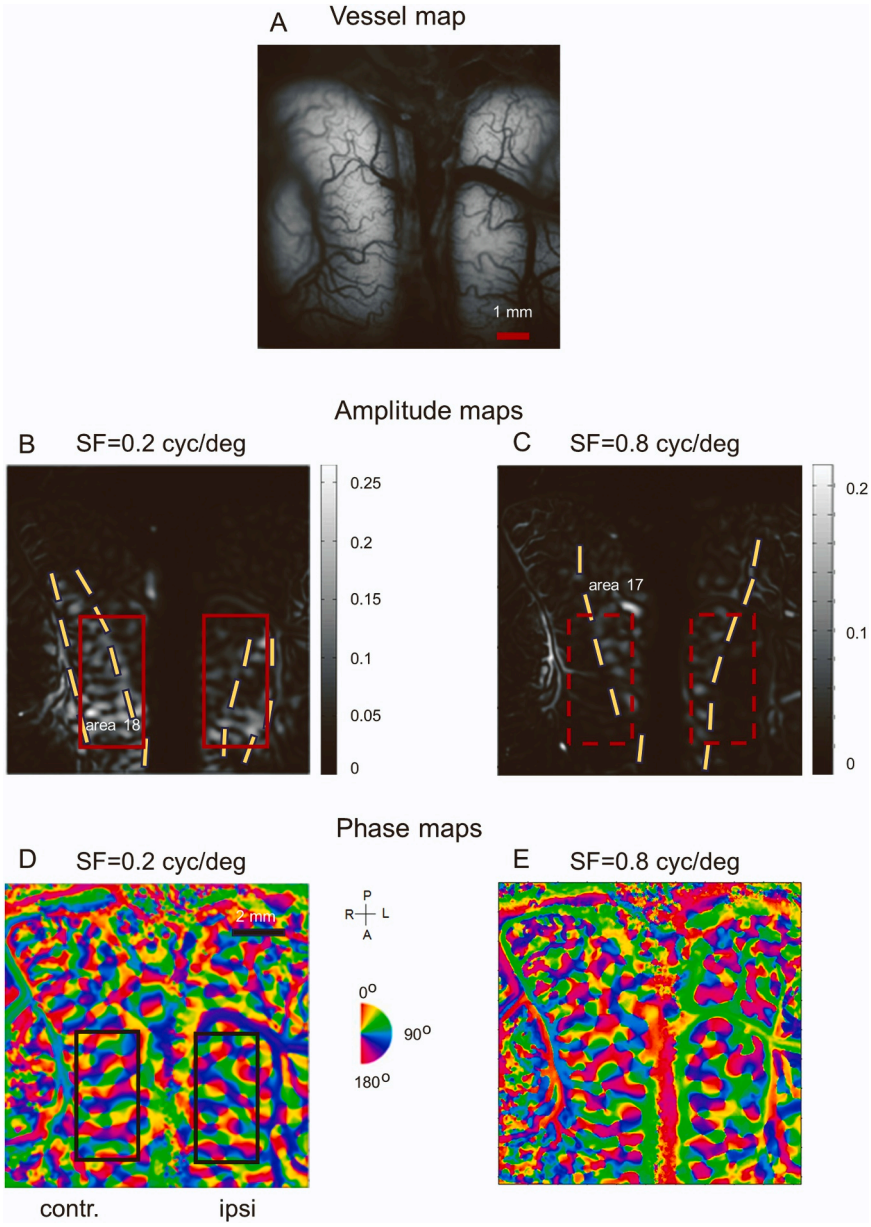

Fig. 2. Selection of ROIs for a subsequent analysis. A, blood vessel pattern of the surface of imaged region shown in B-E obtained with green light (540 nm). Maps of orientation strength (B-C, amplitude maps) and orientation preference (D-E, phase maps) obtained with red light (630 nm) when the camera was focused 600–700 μm below the cortical surface. B, D, maps obtained in response to visual stimulation with a spatial frequency of 0.2 cycles/deg (SF=0.2 cyc/deg). Red (in amplitude maps) and black (in phase maps) rectangles mark region of interest (ROI, 110×200 pixels) of the same size in the contralateral (contr.) and ipsilateral (ipsi) visual cortex. Yellow dashed lines show the limits of the area 18. A, anterior; P, posterior, R, right, L, left. Angle of preferred orientation is displayed in pseudocolor C, E, maps obtained in response to visual stimulation with a spatial frequency of 0.8 cycles/deg (SF=0.8 cyc/deg) which were used to identify the limits of area 17 (yellow dashed lines). Red rectangles with dashed line contour in amplitude maps indicate locations of ROIs for comparison with location of ROIs on the maps obtained with a spatial frequency of 0.2 cyc/deg.

median 0.18 cycles/deg (Issa et al., 2000)). Different properties of neurons in these two visual areas allow to define the border between area 17 and area 18 (Bonhoeffer et al., 1995; Ohki et al., 2000; Fukuda et al., 2006; Liang et al., 2007; Rochefort et al., 2007). A new Fig. 2 shows maps in response to different spatial frequencies. The choice of the region of interest (ROI) depended on several factors. The ROI was chosen to avoid large blood vessels seen in the vessel map (Fig. 2A). The cortex was stimulated with a visual stimulus of 0.2 cycles/deg (orientation amplitude maps and orientation preference maps are shown in Fig. 2 B and D) and 0.8 cycles/deg (Fig. 2C, E). Yellow dashed lines show the limits of the area 18 (Fig. 2B) thus defining the border between area 17 and 18 (Fig. 2B, C). Red (in amplitude maps) and black (in phase maps) rectangles mark region of interest (ROI, 110 ×200 pixels) of the same size in the contralateral (contr.) and ipsilateral (ipsi) visual cortex. The ROIs were selected symmetrically in contralateral and ipsilateral hemispheres (Fig. 2B, D), that is, at the approximately equal distances from the midline and same vertical coordinates. Because we were testing both contralateral and ipsilateral hemispheres for the effect of propofol, the ROI should include both areas 17 and 18 at the location of the transition zone (area 17/18 border along the vertical meridian) where transcallosal fibers and geniculo-cortical fibers converge (Rochefort et al., 2007). The strongest transcallosal activation is achieved with gratings of relatively low spatial and temporal frequencies (Rochefort et al., 2007). Moreover, interhemispheric information transfer is nearly

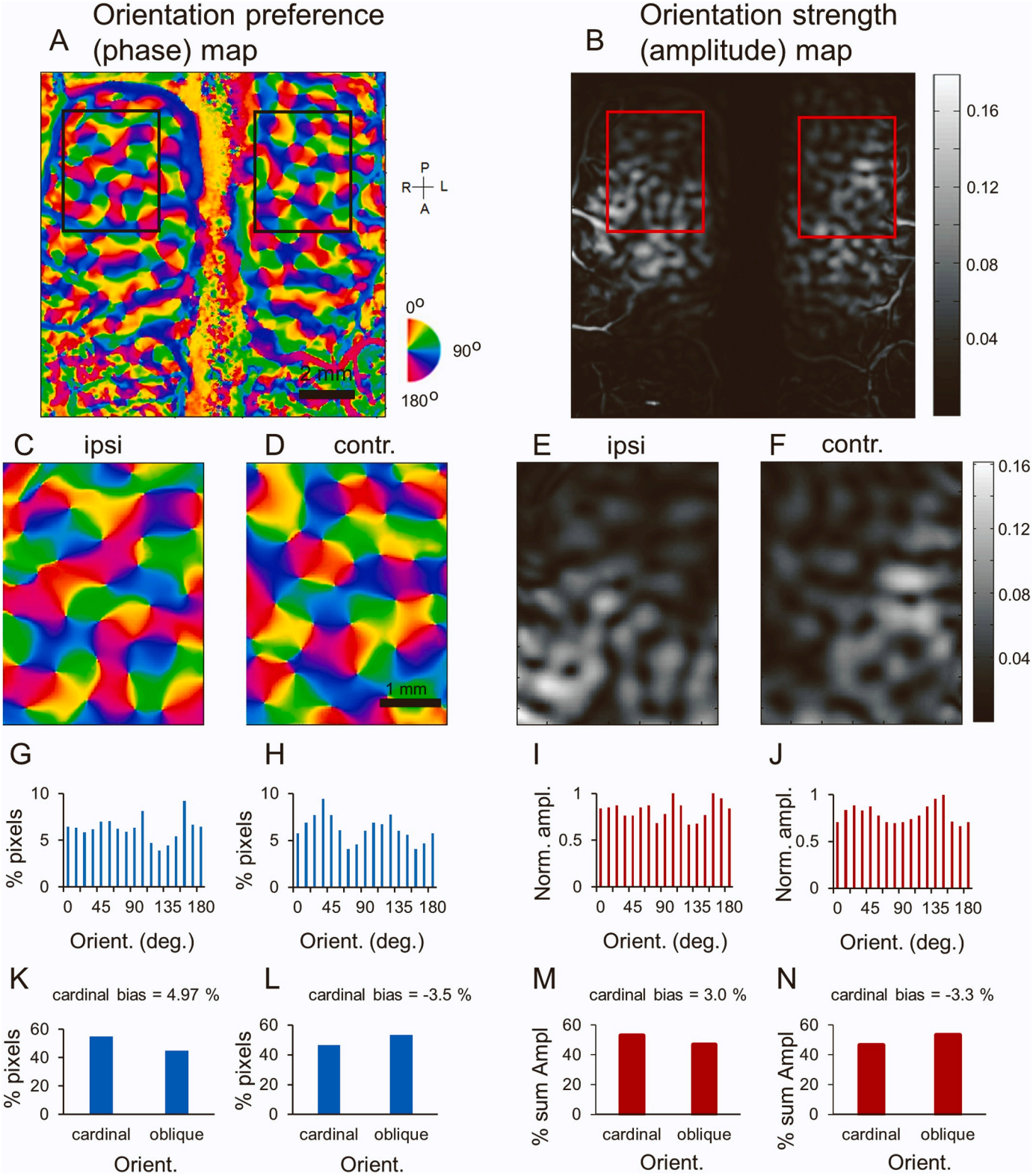

Fig. 3. Maps of orientation preference (A, phase maps) and orientation strength (B, amplitude maps) and their analysis. Rectangles mark region of interest (ROI, 130 ×170 pixels) of the same size in the contralateral (D, F) and ipsilateral (C, E) visual cortex. G-J, orientation map composition. K-L, representation of cardinal (vertical and horizontal) and oblique orientations in ROI. M-N, signal amplitude at cardinal and oblique orientations in ROI. Other conventions as for Fig. 2.

abolished at low contrasts and high spatial and temporal frequencies (Berardi et al., 1987). Finally, it was observed that the highest activation of visual cortex in optical imaging experiments is achieved with the spatial frequency of 0.2 cycles/deg and the temporal frequency of 2 Hz (Kalatsky, 2009). Also, because we studied the effect of propofol on amplitude maps according to cardinal and oblique orientations, the ROI size needed to be large enough to include at least 2–3 iso-orientation domains, the distance between which comprises 1.0–1.1 mm in area

17 and 1.2–1.6 mm in area 18 (Löwel et al., 1987; Fukuda et al., 2006).

The analysis was conducted in MATLAB (Mathworks, Natick, Massachusetts) using custom programs. We calculated two-dimensional correlation coefficients between the control and four consecutive maps. Fig. 3 shows orientation preference (Fig. 3A, C, D) and orientation amplitude maps (Fig. 3B, E, F) and explains the steps of analysis of orientation maps in Control in one of the cats. All pixels in the ROI were divided into 16 bins representing 16 orientations between 0° and 180° with steps of 11.25° and −5.625 - + 5.625° around each orientation. Pixels at 0° (0° −5.625°) and 180° (174.375°- 180°) were joined. We calculated percentage of pixels at each orientation in orientation preference maps (Fig. 3G, H). Then, amplitude of the signal was assessed on corresponding orientations (Fig. 3I, J). Mean amplitude values were calculated at each of 16 orientations and the highest value in the distribution for the contralateral control ("baseline") ROI map (where amplitude was slightly higher in control than in the ipsilateral map) was found. Normalization was done in each cat to this maximum amplitude value that was taken as 1:

$Ampl_{norm\text{-}i} = Ampl_i * 1 / Ampl_{max}$,

where Amp_i is the mean amplitude value at each orientation, $Ampl_{max}$ is the maximum mean amplitude value at one of 16 orientations in the contralateral control ("baseline") ROI map. Normalization is a method that is used by many investigators including those who analyzed results of optical imaging experiments (Bonhoeffer et al., 1995; Dragoi et al., 2001; Basole et al., 2003; Fukuda et al., 2006; Ribot et al., 2013). Normalization removes interindividual variations and allows to directly compare results of different cases.

Cardinal bias (CB) was estimated from orientation distribution histograms as suggested by Coppola and White (2004):

Cardinal bias (%) $= 100 \times$ [cardinal pixels/ (cardinal pixels+oblique pixels)] −50.

Cardinal pixels (representing horizontal and vertical orientation preferences) included 0° (0°-5.625°)−22.5°, 78.75°-101.25°, and 157.5°-180° (174.375°-180°), while oblique pixels included 33.75°-67.5° and 112.5°-146.25°. Thus, an equal number of bins (eight) was devoted to both cardinal and oblique pixels (Fig. 3K, L). Amplitude at cardinal and oblique orientations also was estimated (Fig. 3M, N).

Measurements of changes in each consecutive image within each experiment were compared to the first acquired map at the same pixels. Statistical calculations were done in MATLAB and also with the GB-STAT program (Dynamic Microsystems, USA).

The nonparametric Newman–Keuls' Multiple Comparisons test (N-K test), Wilcoxon Rank Sum/Mann-Whitney U test (U test), and Kruskal-Wallis One-Way ANOVA test (K-W ANOVA test) were used to evaluate differences among groups. The data are presented as mean ± standard error of the mean. Two-tailed t-test was used where appropriate.

3. Results

Altogether, 18 ROIs from 9 cats (2 ROIs for each cat, one in the contralateral hemisphere and another one in the ipsilateral hemisphere) were analyzed. Four cats out of 9 cats used in this study were also used in the experiments described in the previous paper (Shumikhina et al., 2018). As was explained in the "Materials and Methods" section 2.4, we evaluated modifications of orientation maps at different time intervals in 12 min (12 – 24 min, referred as "12 min"), 24 min (24–36 min, referred as "24 min"), 36 min (36–48 min, referred as "36 min"), and 48 min (48–60 min, referred as "48 min") after propofol bolus injections at different doses (2, 3, or 4 mg/kg, 3 animals in each group). The first part (Map-1, 0–12 min, referred as "0 min") was considered as a control.

It has been shown that propofol decreases cerebral oxygen consumption (Marik, 2004) and thus leads to a decrease of the expired CO_2. The common normal physiological parameters maintained during experiments in anesthetized cats are reported in the range 180–220 beats/min for the heart rate (Gillis et al., 1983; Bardy et al., 2006) and 3.7–4.0% for the expired CO_2 (Bardy et al., 2006; Ribot et al., 2013; Meng et al., 2018). Our control parameters were in the same range. Average values for heart rate were 181.2 ± 0.65 beats/min and 4 ± 0.03% for the expired CO_2. We observed a decline of these physiological parameters because of propofol bolus injections. However, no significant differences for all time intervals were revealed. We also calculated cross-correlation coefficients between CO_2, heart rate and amplitude values and found that the correlation coefficients were very low.

3.1. Effect of bolus propofol injection on amplitude map: typical examples

An example of the effect of bolus propofol injection (dose 3 mg/kg) on orientation selectivity maps of a cat primary visual cortex (cat-27) is shown in Fig. 4. This injection decreased the concentration of CO_2 in the expired air from 3.9% to 3.6% (7.7% difference in 7 min after bolus injection). The concentration of CO_2 in the expired air returned to control values in 14 min after injection. Heart rate declined more strongly, from 222 to 171 beats/min (difference 23% in 12 min after bolus injection). The heart rate recovered by 44 min after injection. Correlation coefficients between the control contralateral map and maps recorded 12 min and 24 min later tended to be lower by 11–12% (0.89 and 0.88, respectively) and did not show recovery (Fig. 4A, C). Correlation coefficient between amplitude distributions at different orientations in the contralateral visual cortex (Fig. 4B) decreased by 17% for maps recorded 12 min apart (correlation coefficient was 0.83). For distributions at longer time intervals, the values are: 0.85, 0.88, and 0.91. Correlation coefficients progressively recovered for maps recorded 24–48 min apart (linear fit, $r = 0.99$, $p = 0.0003$, Fig. 4D). Fig. 4E shows the distribution of amplitude values at cardinal and oblique orientations for all time intervals. The y-axis represents the sum of normalized amplitude values over all bins devoted to cardinal or oblique orientations at a given time interval. The correlation coefficient above the plot is the correlation coefficient between distributions of amplitude at cardinal and oblique orientations at different time intervals. There was a high correlation ($r = 0.97$) between the distributions. In this cat, amplitude at cardinal orientations in control contralateral maps was slightly higher (CB=2.1%) than at oblique orientations. The amplitude was decreased in 12 min after injection not equally for cardinal and oblique orientations. This corresponded to an increase in cardinal bias to 3.4%. Fig. 4F shows amplitude changes in comparison with the control map. Immediately after bolus injection, amplitude in the contralateral visual cortex decreased by 21.5% (N-K test, $p < 0.01$). Nearly complete recovery was detected by 48 min after injection with an amplitude value comprising 94.2% from the control (not statistically significant difference between the maps was observed, N-K test, $p > 0.05$).

Similar changes were noticed in the ipsilateral visual cortex (Fig. 4G-L). Correlation coefficients between the control ipsilateral map and maps recorded 24 min apart decreased by 16.6% and partially recovered by 48 min after injection (Fig. 4G, I). Correlation coefficient between amplitude distributions at different orientations (Fig. 4H) decreased by 3–6% not showing recovery (linear fit, $r = -0.99$, $p = 0.008$). Fig. 4K shows the distribution of amplitude values at cardinal and oblique orientations for all time intervals. The y-axis the sum of normalized amplitude values over all bins devoted to cardinal or oblique orientations at a given time interval. The correlation coefficient above the plot is the correlation coefficient between distributions of amplitude at cardinal and oblique orientations at different time intervals. There was a high correlation ($r = 0.99$) between the distributions. In this cat, amplitude at cardinal orientations in control contralateral maps was slightly lower (CB=1.0%) than at oblique orientations. The amplitude was decreased in 12 min after injection not equally for cardinal and oblique orientations. As a result, no preference for cardinal versus oblique orientations were observed for maps recorded 12 min apart (CB=−0.01%) (Fig. 4K). Fig. 4L displays amplitude changes in comparison with a control map. Immediately after bolus injection, amplitude in the ipsilateral visual cortex decreased by 21.1%. These changes

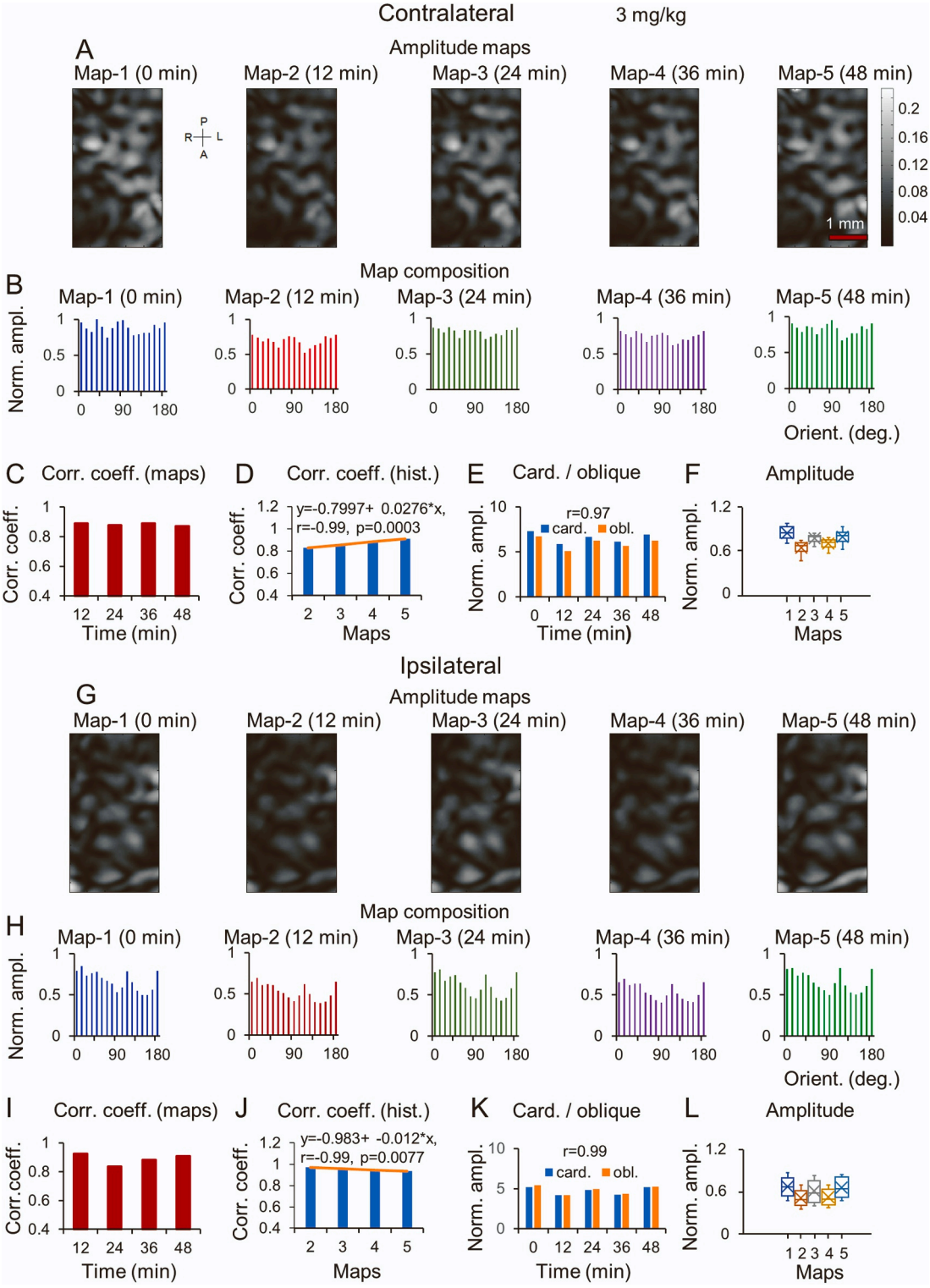

Fig. 4. Changes in orientation selectivity (amplitude) maps observed at different time intervals after propofol bolus (dose 3 mg/kg) in visual cortex in one of the cats. Amplitude maps in contralateral (A) and ipsilateral (G) visual cortex. Amplitude at different orientations in contralateral (B) and ipsilateral (H) visual cortex. Correlation coefficients between amplitude maps in contralateral (C) and ipsilateral (I) visual cortex. Correlation coefficients between distributions of amplitude at different orientations in contralateral (D) and ipsilateral (J) visual cortex. Regression line, equation, coefficient of correlation, and the significance of linear fit of the data are shown on the plot. Amplitude at cardinal and oblique orientations in contralateral (E) and ipsilateral (K) visual cortex. The y-axis represents the sum of normalized amplitude values over all bins devoted to cardinal or oblique orientations at a given time interval. Correlation coefficients between distributions of amplitude at cardinal and oblique orientations are shown in the upper part of the plot. Changes in amplitude at different time intervals after bolus propofol injection in contralateral (F) and ipsilateral (L) visual cortex. Box-and-whiskers plots show median (horizontal line inside of the box), the mean of the data (cross inside of the box), the bottom and top edges of the box indicate the 25th (first quartile, Q1) and 75th (third quartile, Q3) percentiles, and "whiskers" above and below the box show the locations of the minimum and maximum.

were statistically significant (N-K test, $p < 0.01$). Almost complete recovery was seen by 48 min after injection with an amplitude value comprising 98.4% from the control (differences between control maps and maps after 48 min after injection were not statistically significant; N-K test, $p > 0.05$).

Another example of the effect of bolus propofol injection (dose 4 mg/kg) on orientation selectivity maps of a cat primary visual cortex (cat-23) is shown in Fig. 5. This injection decreased the concentration of CO_2 in the expired air from 4.0% to 3.8% (5.0% difference in 2–6 min after bolus injection). The concentration of CO_2 in the expired air returned to control values in 18 min after injection. Heart rate declined more strongly, from 150 to 136 beats/min (9.3% difference in 2 min after bolus injection). The heart rate stayed low till 48 min after injection. Correlation coefficients between the control contralateral map and maps recorded 12 min and 24 min later tended to be lower by 18–22.5% (0.78 and 0.82, respectively) and did not show recovery reaching only a value of 0.88 (Fig. 5A, C). Correlation coefficient between amplitude distributions at different orientations in contralateral visual cortex (Fig. 5B) decreased by 81.7% for maps recorded 12 min apart. Correlation coefficients showed a tendency for recovery for maps recorded 24–48 min apart (linear fit, $r = 0.85$, $p = 0.15$, Fig. 5D). Fig. 5E shows the distribution of amplitude values at cardinal and oblique orientations for all time intervals. The y-axis represents the sum of normalized amplitude values over all bins devoted to cardinal or oblique orientations at a given time interval. The correlation coefficient above the plot is the correlation coefficient between distributions of amplitude at cardinal and oblique orientations at different time intervals. There was a high correlation ($r = 0.98$) between the distributions. In this cat, amplitude at cardinal orientations in control contralateral maps was slightly smaller (CB= −1.3%) than at oblique orientations. The amplitude was decreased in 12 min after injection not equally for cardinal and oblique orientations. This corresponded to an increase in cardinal bias to 2.0%. Fig. 5F shows amplitude changes in comparison with the control map. Immediately after bolus injection, amplitude in the contralateral visual cortex decreased by 45.6% (N-K test, $p < 0.01$). A partial recovery was observed by 48 min after injection (differences between control maps and maps after 48 min after injection comprised 27.1%) (N-K test, $p < 0.01$).

Similar changes were noticed in the ipsilateral visual cortex (Fig. 5G-L). Correlation coefficients between the control ipsilateral map and maps recorded 12 min and 24 min apart decreased by 48.4% and 54.5%, respectively and partially recovered by 48 min after injection (Fig. 5G, I). Correlation coefficient between amplitude distributions at different orientations for maps recorded 12 min apart (Fig. 5H) decreased by 47.8% showing partial recovery (linear fit, $r = -0.94$, $p = 0.0056$). Fig. 5K shows the distribution of amplitude values at cardinal and oblique orientations for all time intervals. The y-axis the sum of normalized amplitude values over all bins devoted to cardinal or oblique orientations at a given time interval. The correlation coefficient above the plot is the correlation coefficient between distributions of amplitude at cardinal and oblique orientations at different time intervals. There was a high correlation ($r = 0.91$) between the distributions. In this cat, amplitude at cardinal orientations in control contralateral maps was lower (CB=−3.0%) than at oblique orientations. The amplitude was decreased in 12 min after injection not equally for cardinal and oblique orientations. As a result, preference for cardinal versus oblique orientations was observed for maps recorded 12 min apart (CB=−5.1%). Fig. 5L displays amplitude changes in comparison with a control map. Immediately after bolus injection, amplitude in the ipsilateral visual cortex decreased by 51.1%. These changes were statistically significant (N-K test, $p < 0.01$). A tendency for recovery was observed by 48 min after injection (differences between control maps and maps after 48 min after injection comprised 40.1%).

3.2. Dose dependency of bolus propofol injection on amplitude maps and interhemispheric differences

In control maps, mean amplitude in 9 cats in the contralateral visual cortex was slightly higher than in the ipsilateral visual cortex (by 14.3%) although the difference was not significant (U test, $p = 0.17$). Amplitude changes after injection of different boluses, averaged across all cats are shown in Fig. 6. In contralateral visual cortex, amplitude of the optical signal at 12 min interval after bolus injection decreased by 21.6% for doses of 2 mg/kg (Fig. 6A), by 35.2% for doses of 3 mg/kg (Fig. 6B), and by 31.4% for doses of 4 mg/kg (Fig. 6C). The differences for all doses were significant (N-K test, $p < 0.01$). At this interval, the effect of the 3 mg/kg bolus was greater than that of the 2 mg/kg one (N-K test, $p < 0.05$) and the effect of the 4 mg/kg bolus was greater than that of the 2 mg/kg one (N-K test, $p < 0.01$). Amplitude increased monotonically at longer time intervals yet did not reach the control level in 48 min after injection for any dose (Fig. 6A-C). In ipsilateral visual cortex, amplitude 12 min after bolus injection decreased by similar values (20.0%) for doses of 2 mg/kg (Figs. 6D) and 3 mg/kg (39.0%, Fig. 6E) but declined more strongly for doses of 4 mg/kg (by 41.4%, Fig. 6F). The differences for all doses were significant (N-K test, D, F, $p < 0.01$, E, $p < 0.01$ for 12–36 min and $p < 0.05$ for 48 min). Amplitude increased monotonically at longer time intervals but did not recover in full in 48 min after bolus injection (Fig. 6D-F). At this interval, the effect of the 3 mg/kg bolus was greater than that of the 2 mg/kg one (N-K test, $p < 0.01$) and the effect of the 4 mg/kg bolus was greater than that of the 2 mg/kg one (N-K test, $p < 0.01$).

3.3. Effect of bolus propofol injection: amplitude changes at different orientations

The effect of bolus propofol injections is demonstrated also in Fig. 7 where amplitude changes are shown at different stimulus orientations. As can be seen on each plot, the curves look similar at different time intervals (intervals are color-coded) in spite of amplitude decline, both in contralateral (Fig. 7A-C) and ipsilateral (Fig. 7D-F) visual cortex. High correlation coefficients were revealed between curves at different time intervals for all doses and different hemispheres, usually varying from 0.8 to 0.9 (N-K test, $p < 0.05$ to $p < 0.0001$). For all propofol boluses, amplitude maximum in curves usually appeared at the same orientations as in control. In the control, no differences between curves in the contralateral and ipsilateral hemispheres were found for a dose of 2 mg/kg. The curves in control for doses of 3 mg/kg and 4 mg/kg were significantly different (N–K test, $p < 0.01$). For a dose of 2 mg/kg, the distributions were not significantly different at the 12 min time interval after bolus injection. It means that administration of propofol affected equally both hemispheres. Curves also were similar for the 48 min time interval after bolus injection. For doses of 3 mg/kg and 4 mg/kg, amplitude values in the contralateral and ipsilateral hemispheres were significantly different at all time intervals (N–K test, $p < 0.01$).

Amplitude changes at different orientations after different bolus propofol injections are further demonstrated in Fig. 8. We observed a large difference between cats regarding the cardinal bias. In control conditions, amplitude in the contralateral visual cortex was higher at cardinal orientations in 5 out of 9 cats with a cardinal bias varying from 0.5 to 5.8%. In 4 other cats, the cardinal bias was negative, that is, amplitude was higher at oblique orientations (−0.3 to −3.3%). In the ipsilateral visual cortex, amplitude was higher at cardinal orientations in 4 out of 9 cats varying from 0.7 to 8.4%. In other 5 cats, amplitude was higher at oblique orientations (−0.3 to −3.0%). Overall, in 9 cats in control condition amplitude at cardinal orientations was higher than at oblique orientations by 2.2% in the contralateral visual cortex and by 0.3% in the ipsilateral visual cortex. However, the differences were not significant (two-tailed t-test, $p = 0.51$ and $p = 0.96$, respectively).

There were 3 animals in each group for each dose. The analysis was executed independently on the positive or negative cardinal bias. In

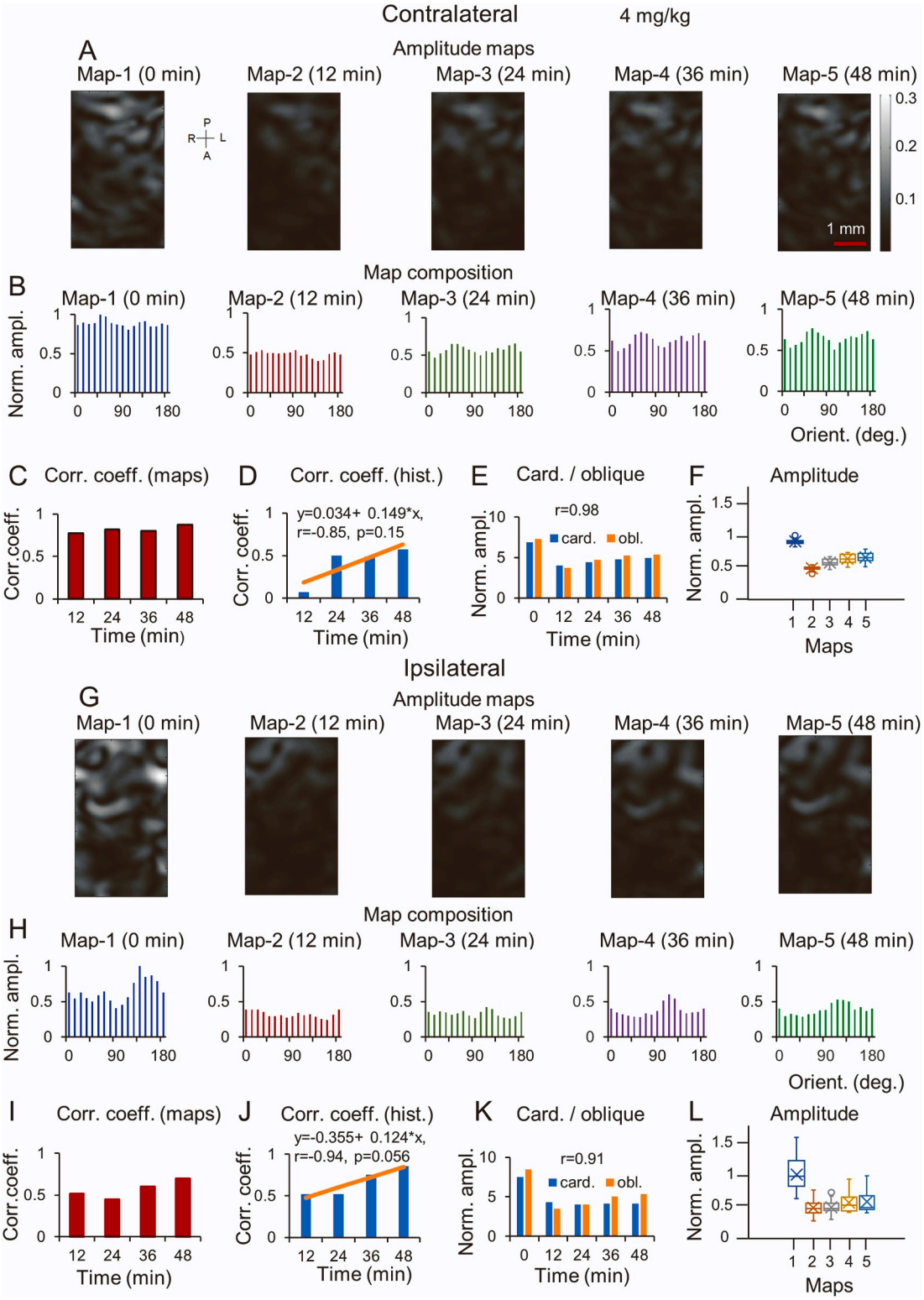

Fig. 5. Changes in orientation selectivity (amplitude) maps observed at different time intervals after propofol bolus (dose 4 mg/kg) in visual cortex in one of the cats. Amplitude maps in contralateral (A) and ipsilateral (G) visual cortex. Amplitude at different orientations in contralateral (B) and ipsilateral (H) visual cortex. Correlation coefficients between amplitude maps in contralateral (C) and ipsilateral (I) visual cortex. Correlation coefficients between distributions of amplitude at different orientations in contralateral (D) and ipsilateral (J) visual cortex. Amplitude at cardinal and oblique orientations in contralateral (E) and ipsilateral (K) visual cortex. Changes in amplitude at different time intervals after bolus propofol injection in contralateral (F) and ipsilateral (L) visual cortex. Box-and-whiskers plots show median (horizontal line inside of the box), the mean of the data (cross inside of the box), the bottom and top edges of the box indicate the 25th (first quartile, Q1) and 75th (third quartile, Q3) percentiles, and "whiskers" above and below the box show the locations of the minimum and maximum. Other conventions as for Fig. 4.

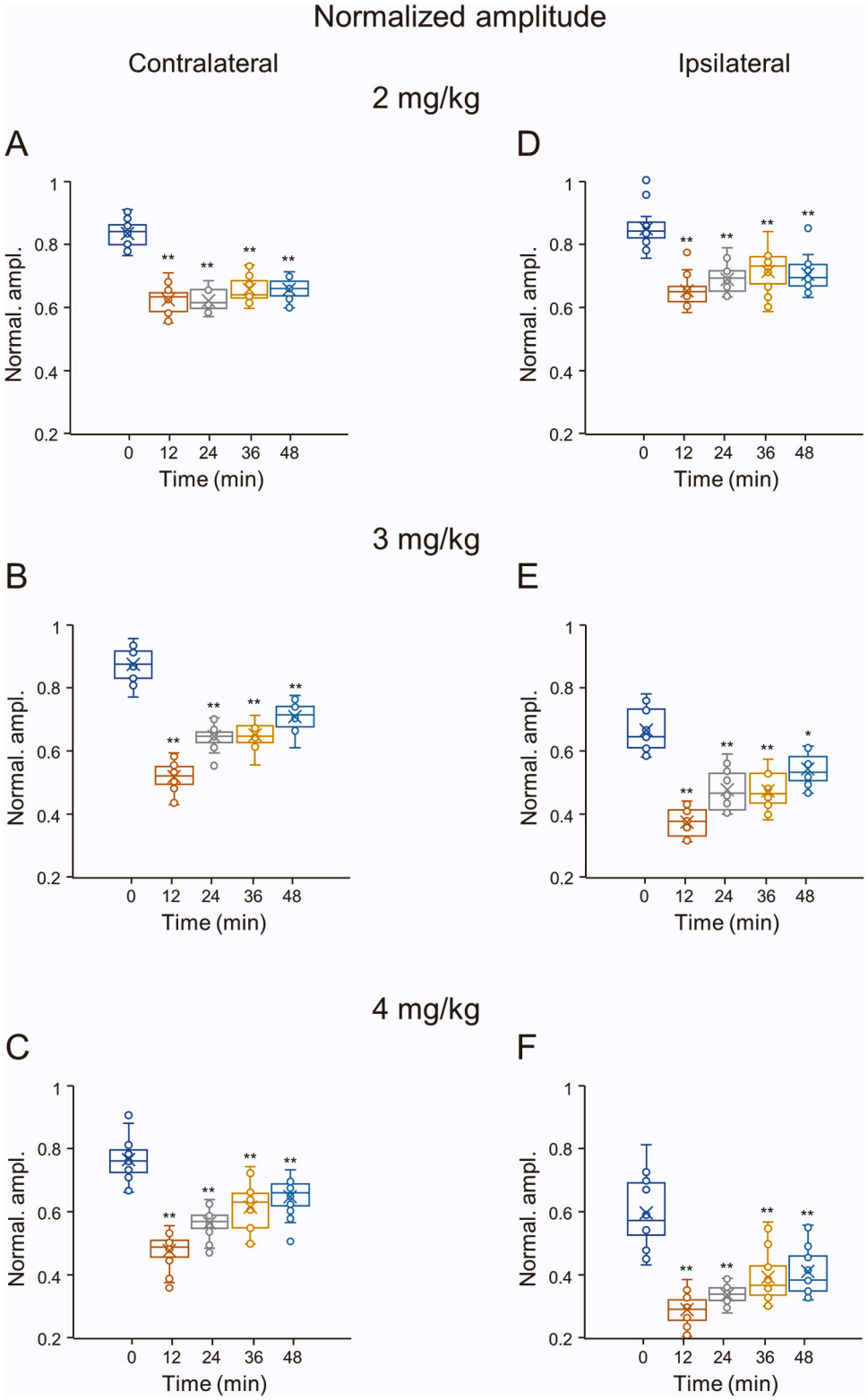

Fig. 6. Modifications of amplitude of optical signals recorded continuously for 1 h after injection of bolus dose of propofol. Box-and-whiskers plots show amplitude changes in contralateral (A-C) and ipsilateral (D-F) visual cortex at different bolus propofol doses. Dots represent outliers. Stars indicate significant changes in relation to control (*, $p < 0.05$, **, $p < 0.01$). Other conventions as for Fig. 4.

other words, each group included animals with both positive and negative cardinal bias. No differences were found between amplitude modifications at cardinal and oblique orientations in either contralateral (Fig. 8A) or ipsilateral (Fig. 8C) visual cortex, except for amplitude changes in the contralateral cortex at the 2 mg/kg dose (Fig. 8A, K-W ANOVA test, $p < 0.05$). However, the distribution of amplitude values at cardinal orientations in the contralateral cortex was significantly different from the distribution in the ipsilateral hemisphere (N-K test, $p < 0.05$ at the dose of 2 mg/kg; $p < 0.01$ at the dose of 3 mg/kg, and $p < 0.05$ at the dose of 4 mg/kg). In the latter, amplitude at cardinal

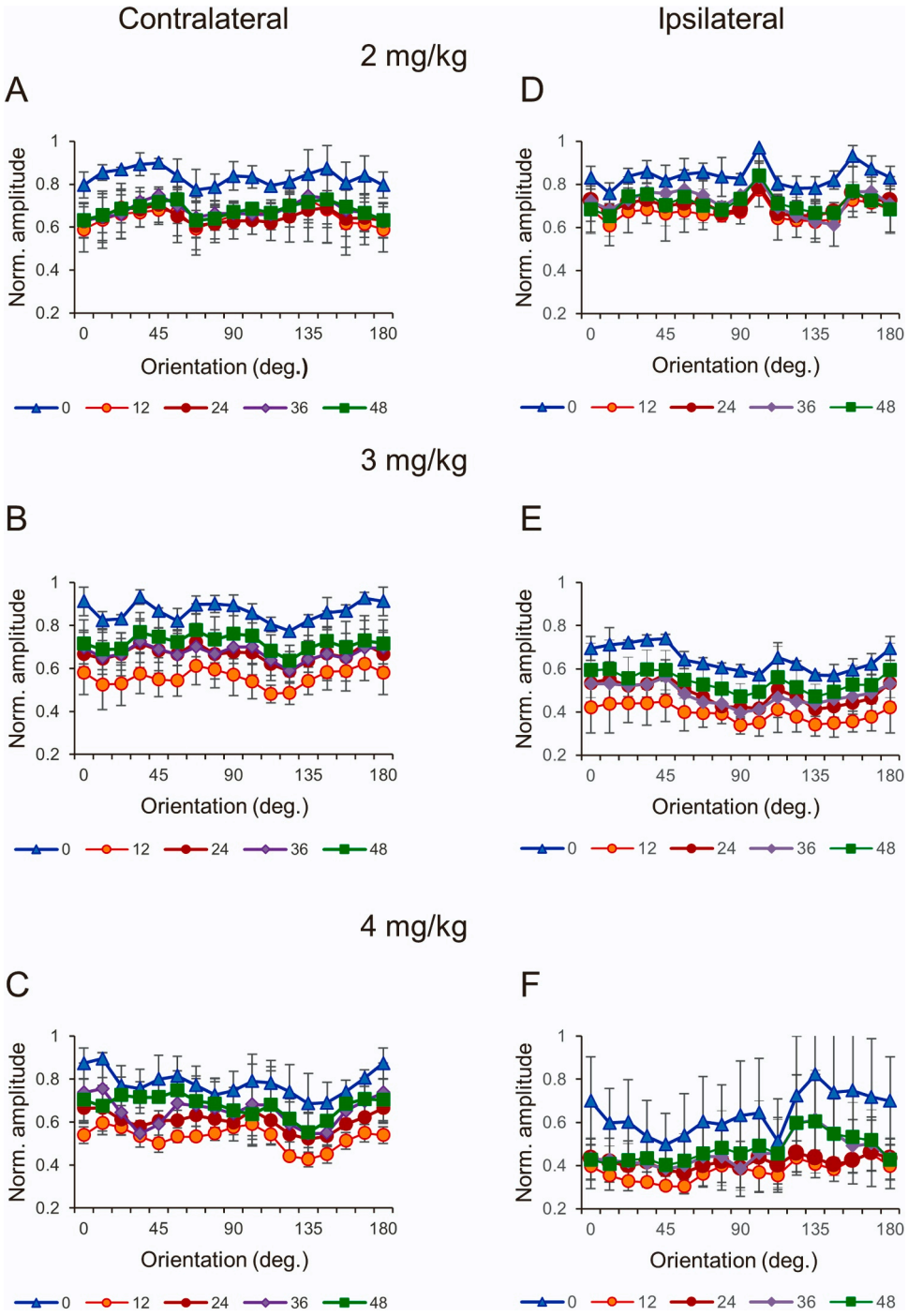

Fig. 7. Changes in amplitude of optical signals at different orientations and different propofol doses and time intervals. A-C, changes in contralateral visual cortex. D-F, changes in ipsilateral visual cortex. Time intervals (0, 12, 24, 36, 48 min) are color-coded.

orientations was depressed stronger at most time intervals after bolus injection at doses of 3 mg/kg and 4 mg/kg. Amplitude at oblique orientations was significantly lower in the ipsilateral cortex at the dose of 3 mg/kg (N-K test, $p < 0.05$).

Changes in the absolute cardinal bias values are shown in Fig. 8B and D. Average values for 3 cats in each group (according to 3 different doses) are used for the comparison for which the statistics is indicated. There was no significant difference between cardinal bias values within each group (i.e., each dose) at neither time interval, neither in the contralateral or ipsilateral visual cortex. No significant differences were observed for distributions of absolute cardinal bias values (when a sign of cardinal bias is not a factor) at different doses in the contralateral visual cortex (Fig. 8B). Significant differences were only revealed, if not absolute but original values (with positive and negative cardinal bias) were compared. In the latter case, the significant differences were observed between cardinal bias values at doses of 2 and 3 mg/kg (N-K test, $p < 0.05$) and 2 and 4 mg/kg (N-K test, $p < 0.01$). No significant difference was observed between distributions of cardinal bias values at 3 and 4 mg/kg doses, when original cardinal bias values were compared. In the ipsilateral visual cortex (Fig. 8D), significant differences were seen for distributions of absolute cardinal bias values at doses of 2 and 3 mg/kg (N-K test, $p < 0.01$) and 3 and 4 mg/kg (N-K test, $p < 0.01$). No significant differences were found between distributions of amplitude values at vertical and horizontal orientations at different doses and

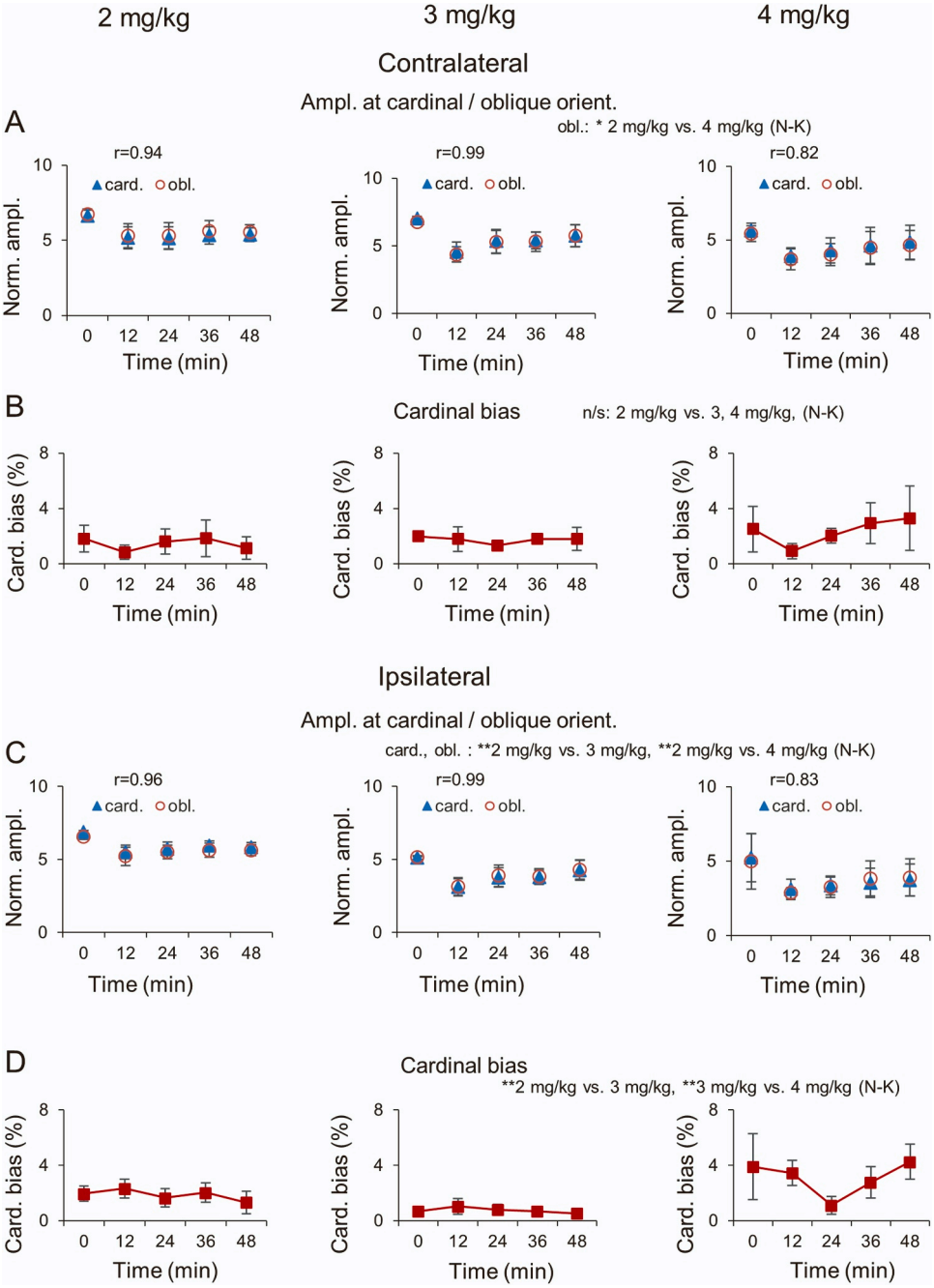

Fig. 8. Alterations in amplitude of optical signals recorded at cardinal and oblique orientations and different propofol doses and time intervals. A-B, changes in contralateral visual cortex. C-D, changes in ipsilateral visual cortex. A and C, amplitude distributions at cardinal and oblique orientations. The y-axis represents the sum of normalized amplitude values over all bins devoted to cardinal or oblique orientations at a given time interval. Correlation coefficients above the plots are the correlation coefficients between distributions of amplitude at cardinal and oblique orientations at different time intervals. B and D, cardinal bias values for amplitude changes. The statistically significant differences are indicated above the plots.

between different hemispheres.

4. Discussion

Here, we show that a bolus dose of propofol leads to a marked decrease in the amplitude of optical signal in visual cortex and that this effect is dose-dependent.

4.1. Dose dependency of propofol effects

The dose dependency of the effects of propofol on cortical activity *in vivo* was reported by different investigators in studies performed mostly in rats and humans (Antunes et al., 2003; Logginidou et al., 2003; Dueck et al., 2005; Reed and Plourde, 2015). In cats, previous reports of our group have shown that bolus injections of a propofol leads to a depression of amplitude of optical signals by 40% (Bugrova et al., 2013; Bugrova and Bondar', 2019). Here, we analyzed the effect of propofol bolus injection depending on its dose. We have found a clear dose dependency of the effects.

Single intravenous bolus injections of propofol are used for induction of anesthesia and for a fast deepening the anesthetic depth when needed on the background of a continuous infusion. In our experiments, we

replicated the last condition. It means that animals already had some anesthetic level of propofol before bolus injections. We deepened the anesthesia injecting propofol bolus at different doses (2, 3, or 4 mg/kg).

In medicine, the suggested induction propofol bolus dose for adults is 2–2.5 mg/kg (Cummings et al., 1984; Briggs and White, 1985; Kay et al., 1985; Reilly and Nimmo, 1987; Langley and Heel, 1988). In premedicated cats, as in our case, induction doses were suggested from 3 to 5 mg/kg (Glowaski and Wetmore, 1999; Hall et al., 1999; Weaver and Raptopoulos, 1990) or even from 6 mg/kg to 8 mg/kg (Morgan and Legge, 1989; Geel, 1991; Taboada and Murison, 2010; Taylor et al., 2012; Griffenhagen et al., 2015). Thus, the bolus doses that we used were similar order considering that bolus doses in our study were injected on the background of a continuous infusion.

The precise dose-response relationships are not easy to establish because of different experimental protocols and rather large variability between individual animals (Bonhomme et al., 2019).

Optical imaging experiments are based on recordings of scattered light changes related to neurophysiological activity. There is a good correlation between the amplitude of optical signal and both spike firing and subthreshold synaptic potentials (Das and Gilbert, 1995). Thus, the method of optical imaging is useful for the evaluation of the dose-dependency of propofol.

The graded dose-dependent reduction of amplitude of the optical signal suggests different sensitivity of various subtypes of cortical neurons to the propofol action. For example, it was observed in the rat insular cortical slice preparation that spike firing in pyramidal (excitatory) neurons was more suppressed by propofol than that of GABAergic fast-spiking neurons. Moreover, the activity of pyramidal neurons decreased at lower propofol concentrations than firing of GABAergic neurons (Kaneko et al., 2016).

A question of recovery after propofol bolus injection is related to the question about dose-dependency of propofol effects. Our previous experiments have shown that orientation maps are rather stable over time (Shumikhina et al., 2018). Thus, there is a very small probability for progressive deterioration in the health of the brain to occur during one hour of recordings. However, as we noticed in Method section, "maps recorded over a period of more than one hour could show some instability (Shumikhina et al., 2018). Thus, some processes occurring after one hour of stimulation could interfere with effects of the bolus propofol injection and hence were avoided by limiting the data collection period to 1 h only". As was reported by Langley and Heel (1988), the elimination half-life of propofol in dogs and cats is usually about 100 min and a terminal elimination half-life is 184–309 min following single doses of propofol. Morgan and Legge (1989) informed that cats were alert and able to stand in 27–38 min after induction dose of propofol. Other authors (Pascoe et al., 2006), however, have found that the ability of cats to walk without ataxia occurs in 80 ± 15 min after anesthetic induction with propofol. The latter results correspond to our findings in the sense that recovery from propofol bolus injections may occur in 60 or more minutes after injection.

The question about the possible saturation of the effect is left unanswered in our study. This is because of limitations of used method of optical imaging in the sense that higher doses of propofol bolus could produce a stronger suppression of cortical activity that may not allow to record reliable maps. Nevertheless, because we did not find a significant difference in the amplitude values between doses of 3 and 4 mg/kg, this may be attributed to a possible saturation of the effect already under the dose of 4 mg/kg. However, possible interindividual differences also should be taken into account.

The method of optical imaging of intrinsic signals can be used for all species. The effect of propofol administration on orientation amplitude maps should be similar across species in the sense of the dose dependency of the effect. However, because anesthetic propofol doses are different for different animals, the dependence on the dose should be estimated in each case.

4.2. Interhemispheric differences

Under monocular stimulation, the contralateral cortex receives crossed in the chiasm pathways from nasal part of the retina through the direct geniculocortical projections while the ipsilateral cortex is activated by uncrossed in the chiasm information from the temporal part of the retina. The proportion of crossed fibers in cats is higher (57%) than of uncrossed ones (43%) (Aebersold et al., 1981). Hence, it may be expected that the stimulation of contralateral pathway will give a stronger response. Indeed, in our experiments there was some tendency for mean amplitude in control maps in the contralateral visual cortex to be higher than in the ipsilateral visual cortex although the difference did not reach the level of statistical significance. However, both hemispheres communicate by callosal fibers (Berlucchi and Rizzolatti, 1968). Transcallosal pathways are limited by the transition zone between area 17 and area 18 where the central vertical meridian is projected. The extent of the transition zone depends on the visual elevation (Payne, 1990) increasing with decreasing visual elevation (Payne, 1990; Berman and Grant, 1992). Transcallosal fibers provide additional activation of the ipsilateral cortex for matching orientations (Rochefort et al., 2007) thus augmenting the response evoked through uncrossed pathways. However, composition of crossed and uncrossed pathways is different. The latter include mostly Y and W cells while more X cells project contralaterally (Stone and Fukuda, 1974) that may lead to different response stability in the ipsilateral and contralateral cortex. This is because X cells are small and have properties distinct from Y and W cells.

While for doses of 2 mg/kg and 3 mg/kg the depression of amplitude in our study was nearly similar between contralateral and ipsilateral visual cortex, some differences were seen between them for the 4 mg/kg doses. For this dose, amplitude decline had a tendency to be stronger in the ipsilateral cortex reaching 41.4% in comparison with 31.4% albeit the difference did not reach the level of statistical significance (t-test, $p = 0.28$).

4.3. Cardinal bias

It is generally accepted that more cortical cells and thus larger cortical areas respond to cardinal (vertical and horizontal) orientations of visual stimuli, both in humans and animals (the so-called "oblique effect"). In cats, the effect was also described although some authors did not find a clear difference between cortical representations of cardinal and oblique angles (Hubel and Wiesel, 1962; Campbell et al., 1968; Rose and Blakemore, 1974). However, some authors pointed out that the anisotropies were seen clearly only in the foveal region (Leventhal and Hirsch, 1977; Kennedy and Orban, 1979; Orban and Kennedy, 1981). Thus, the results would depend on the location of ROIs. In our experiments, we were concentrated not on the orientation preferences but on amplitude changes at different orientations. Yu and Shou (2000) shortly reported that cardinal stimuli evoked greater intrinsic optical signals in comparison with responses evoked by oblique stimuli in cats but no details were provided. In general, our data are consistent with the above findings. However, we found only slight differences between amplitude values at cardinal and oblique orientations in control condition. After propofol bolus injection, the distribution of amplitude values at cardinal orientations in the contralateral cortex was significantly different from the distribution in the ipsilateral hemisphere. In the latter, amplitude at cardinal orientations was depressed stronger at most time intervals after bolus injection at doses of 3 mg/kg and 4 mg/kg. However, we had limited sample sizes.

Propofol should similarly affect the amplitude values at cardinal and oblique orientations in different species because of a common design for the layout of orientation columns (Kaschube et al., 2010) in spite that some animals (for example, tree shrews and galagos) lack orientation columns. The question of anisotropy in the amplitude values at cardinal and oblique orientations may need a further investigation.

Overall, because cortex activity is greatly affected by bolus propofol

injections it is not recommended to continue data collection immediately after bolus injections.

CRediT authorship contribution statement

Svetlana I. Shumikhina: Conceptualization, Investigation, Software, Formal analysis, Visualization, Writing – original draft. **Sergei A. Kozhukhov:** Investigation, Data curation. **Igor V. Bondar:** Methodology, Investigation, Supervision.

Acknowledgments

This research was supported within the state assignment of Ministry of Education and Science of the Russian Federation for 2021-2023 (No. AAAA-A17-117092040002-6).

Conflict of Interest

The authors declare no competing financial interests.

References

Aebersold, H., Creutzfeldt, O.D., Kuhnt, U., Sanides, D., 1981. Representation of the visual field in the optic tract and optic chiasma of the cat. Exp. Brain Res. 42, 127–145. https://doi.org/10.1007/BF00236900.

Alitto, H.J., Dan, Y., 2010. Function of inhibition in visual cortical processing. Curr. Opin. Neurobiol. 20, 340–346. https://doi.org/10.1016/j.conb.2010.02.012.

Antunes, L.M., Roughan, J.V., Flecknell, P.A., 2003. Effects of different propofol infusion rates on EEG activity and AEP responses in rats. J. Vet. Pharmacol. Ther. 26, 369–376. https://doi.org/10.1046/j.1365-2885.2003.00499.x.

Arena, A., Lamanna, J., Gemma, M., Ripamonti, M., Ravasio, G., Zimarino, V., De Vitis, A., Beretta, L., Malgaroli, A., 2017. Linear transformation of the encoding mechanism for light intensity underlies the paradoxical enhancement of cortical visual responses by sevoflurane. J. Physiol. 595, 321–339 https://doi.org/: 10.1113/JP272215.

Bardy, C., Huang, J.Y., Wang, C., FitzGibbon, T., Dreher, B., 2006. Simplification' of responses of complex cells in cat striate cortex: suppressive surrounds and 'feedback' inactivation. J. Physiol. 574 (3), 731–750. https://doi.org/10.1113/jphysiol.2006.110320.

Basole, A., White, L.E., Fitzpatrick, D., 2003. Mapping multiple features in the population response of visual cortex. Nature 423, 986–990.

Berardi, N., Bisti, S., Maffei, L., 1987. The transfer of visual information across the corpus callosum: spatial and temporal properties in the cat. J. Physiol. 384, 619–632. https://doi.org/10.1113/jphysiol.1987.sp016473.

Berlucchi, G., Rizzolatti, G., 1968. Binocularly driven neurons in visual cortex of split-chiasm cats. Science 159, 308–310. https://doi.org/10.1126/science.159.3812.308.

Berman, N.E., Grant, S., 1992. Topographic organization, number, and laminar distribution of callosal cells connecting visual cortical areas 17 and 18 of normally pigmented and Siamese cats. Vis. Neurosci. 9, 1–19. https://doi.org/10.1017/s0952523800006337.

Bonhoeffer, T., Grinvald, A., 1991. Iso-orientation domains in cat visual cortex are arranged in pinwheel-like patterns. Nature 353, 429–431. https://doi.org/10.1038/353429a0.

Bonhoeffer, T., Grinvald, A., 1993. The layout of iso-orientation domains in area 18 of cat visual cortex: optical imaging reveals a pinwheel-like organization. J. Neurosci. 13, 4157–4180. https://doi.org/10.1523/JNEUROSCI.13-10-04157.1993.

Bonhoeffer, T., Kim, D.S., Malonek, D., Shoham, D., Grinvald, A., 1995. Optical imaging of the layout of functional domains in area 17 and across the area 17/18 border in cat visual cortex. Eur. J. Neurosci. 7, 1973–1988. https://doi.org/10.1111/j.1460-9568.1995.tb00720.x.

Bonhomme, V., Staquet, C., Montupil, J., Defresne, A., Kirsch, M., Martial, C., Vanhaudenhuyse, A., Chatelle, C., Larroque, S.K., Raimondo, F., Demertzi, A., Bodar, t O., Laureys, S., Gosseries, O., 2019. General anesthesia: a probe to explore consciousness. Front. Syst. Neurosci. published: 14 August 2019. https://doi.org/10.3389/fnsys.2019.00036.

Briggs, L.P., White, M., 1985. The effects of premedication on anaesthesia with propofol ('Diprivan'). Postgrad. Med. J. 61 (Suppl. 3), 35–37.

Brown, H.A., Allison, J.D., Samonds, J.M., Bonds, A.B., 2003. Nonlocal origin of response suppression from stimulation outside the classic receptive field in area 17 of the cat. Vis. Neurosci. 20, 85–96 https://doi.org/10.1017S0952523803201097.

Buggy, D.J., Nicol, B., Rowbotham, D.J., Lambert, D.G., 2000. Effects of intravenous anesthetic agents on glutamate release: a role for GABAA receptor-mediated inhibition. Anesthesiology 92, 1067–1073. https://doi.org/10.1097/00000542-200004000-00025.

Bugrova, V.S., Bondar, I.V., 2019. Sustainability of the orientational and directional functional domains in the primary visual cortex of cat to the impact of propofol. Zh. Vyss. Nerv. Deyat. Im. I. P. Pavlov. 69, 218–229.

Bugrova, V.S., Ivanov, R.S., Bondar, I.V., 2013. Effect of propofol on functional response of neuronal population in cat primary visual cortex. Ross. Fiziol. Zh. Im. I. M. Sechenova 99, 453–463.

Campbell, F.W., Cleland, B.G., Cooper, G.F., Enroth-Cugell, C., 1968. The angular selectivity of visual cortical cells to moving gratings. J. Physiol. 198, 237–250. https://doi.org/10.1113/jphysiol.1968.sp008604.

Cavazzuti, M., Porro, C.A., Barbieri, A., Galetti, A., 1991. Brain and spinal cord metabolic activity during propofol anaesthesia. Br. J. Anaesth. 66, 490–495. https://doi.org/10.1093/bja/66.4.490.

Chen, X., Shu, S., Bayliss, D.A., 2005. Suppression of Ih contributes to propofol-induced inhibition of mouse cortical pyramidal neurons. J. Neurophysiol. 94, 3872–3883. https://doi.org/10.1152/jn.00389.2005.

Collins, G.G.S., 1988. Effects of the anaesthetic 2,6-diisopropylphenol on synaptic transmission in the rat olfactory cortex slice. Br. J. Pharmacol. 95, 939–949.

Concas, A., Santoro, G., Mascia, M.P., Serra, M., Sanna, E., Biggio, G., 1990. The general anesthetic propofol enhances the function of gamma-aminobutyric acid-coupled chloride channel in the rat cerebral cortex. J. Neurochem. 55, 2135–2138. https://doi.org/10.1111/j.1471-4159.1990.tb05807.x.

Coppola, D.M., White, L., 2004. Visual experience promotes the isotropic representation of orientation preference. Vis. Neurosci. 21, 39–51. https://doi.org/10.1017/s0952523804041045.

Coppola, D.M., White, L.E., Fitzpatrick, D., Purves, D., 1998. Unequal representation of cardinal and oblique contours in ferret visual cortex. Proc. Natl. Acad. Sci. U.S.A. 95, 2621–2623. https://doi.org/10.1073/pnas.95.5.2621.

Craddoc, R., Vasalauskaite, A., Ranson, A., Sengpiel, F., 2023. Experience dependent plasticity of higher visual cortical areas in the mouse. Cereb. Cortex 33, 9303–9312. https://doi.org/10.1093/cercor/bhad203.

Cummings, G.C., Dixon, J., Kay, N.H., Windsor, J.P.W., Major, E., et al., 1984. Dose requirements of ICI 35,868 (propofol, 'Diprivan') in a new formulation for induction of anaesthesia. Anaesthesia 39, 1168–1171. https://doi.org/10.1111/j.1365-2044.1984.tb06425.x.

Das, A., Gilbert, C.D., 1995. Long-range horizontal connections and their role in cortical reorganization revealed by optical recording of cat primary visual cortex. Nature 375, 780–784. https://doi.org/10.1038/375780a0.

Debanne, D., Campanac, E., Bialowas, A., Carlier, E., Alcaraz, G., 2011. Axon physiology. Physiol. Rev. 91, 555–602. https://doi.org/10.1152/physrev.00048.2009.

Dragoi, V., Turcu, C.M., Sur, M., 2001. Stability of cortical responses and the statistics of natural scenes. Neuron 32, 1181–1192. https://doi.org/10.1016/s0896-6273(01)00540-2.

Dueck, M.H., Petzke, F., Gerbershagen, H.J., Paul, M., Hesselmann, V., Girnus, R., Krug, B., Sorger, B., Goebel, R., Lehrke, R., Sturm, V., Boerner, U., 2005. Propofol attenuates responses of the auditory cortex to acoustic stimulation in a dose-dependent manner: a FMRI study. Acta Anaesthesiol. Scand. 49, 784–791. https://doi.org/10.1111/j.1399-6576.2005.00703.x.

Dunn, T., Mossop, D., Newton, A., Gammon, A., 2007. Propofol for procedural sedation in the emergency department. Emerg. Med. J. 24, 459–461. https://doi.org/10.1136/emj.2007.046714.

Ferster, D., Miller, K.D., 2000. Neural mechanisms of orientation selectivity in the visual cortex. Annu. Rev. Neurosci. 23, 441–471. https://doi.org/10.1146/annurev.neuro.23.1.441.

Fritschy, J.-M., Panzanelli, P., 2014. $GABA_A$ receptors and plasticity of inhibitory neurotransmission in the central nervous system. Eur. J. Neurosci. 39, 1845–1865. https://doi.org/10.1111/ejn.12534.

Frostig, R.D., Lieke, E.E., Ts'o, D.Y., Grinvald, A., 1990. Cortical functional architecture and local coupling between neuronal activity and the microcirculation revealed by *in vivo* high-resolution optical imaging of intrinsic signals. Proc. Natl. Acad. Sci. USA 87, 6082–6086. https://doi.org/10.1073/pnas.87.16.6082.

Fukuda, M., Moon, C.-H., Wang, P., Kim, S.-G., 2006. Mapping iso-orientation columns by contrast agent-enhanced functional magnetic resonance imaging: reproducibility, specificity, and evaluation by optical imaging of intrinsic signal. J. Neurosci. 26, 11821–11832. https://doi.org/10.1523/JNEUROSCI.3098-06.2006.

Funahashi, M., Higuchi, H., Miyawaki, T., Shimada, M., Matsuo, R., 2001. Propofol suppresses a hyperpolarization-activated inward current in rat hippocampal CA1 neurons. Neurosci. Lett. 311, 177–180. https://doi.org/10.1016/s0304-3940(01)02169-3.

Geel, J.K., 1991. The effect of premedication on the induction dose of propofol in dogs and cats. J. S. Afr. Vet. Assoc. 62, 118–123.

Gillis, R.A., Quest, J.A., Pagani, F.D., Souza, J.D., Da Silva, A.M., Jensen, R.T., Garvey 3rd, T.Q., Hamosh, P., 1983. Activation of central nervous system cholecystokinin receptors stimulates respiration in the cat. J. Pharmacol. Exp. Ther. 224, 408–414.

Glowaski, M.M., Wetmore, L.A., 1999. Propofol: application in veterinary sedation and anesthesia. Clin. Techn. Small Anim. Pract. 14, 1–9. https://doi.org/10.1016/S1096-2867(99)80021-8.

Griffenhagen, G.M., Rezende, M.L., Gustafson, D.L., 2015. Pharmacokinetics and pharmacodynamics of propofol with or without 2% benzyl alcohol following a single induction dose administered intravenously in cats. Vet. Anaesth. Analg. 42, 472–483. https://doi.org/10.1111/vaa.12233.

Grinvald, A., Frostig, R.D., Siegel, R.M., Bartfeld, E., 1991. High-resolution optical imaging of functional brain architecture in the awake monkey. Proc. Natl. Acad. Sci. USA 88, 11559–11563. https://doi.org/10.1073/pnas.88.24.11559.

Grinvald, A., Lieke, E.E., Frostig, R.D., Hildesheim, R., 1994. Cortical point-spread function and long-range lateral interactions revealed by real-time optical imaging of macaque monkey primary visual cortex. J. Neurosci. 14, 2545–2568. https://doi.org/10.1523/JNEUROSCI.14-05-02545.1994.

Grinvald, A., Lieke, E., Frostig, R.D., Gilbert, C.D., Wiesel, T.N., 1986. Functional architecture of cortex revealed by optical imaging of intrinsic signals. Nature 324, 361–364. https://doi.org/10.1038/324361a0.

Hall, T.L., Duke, T., Townsend, H.G.C., Caulkett, N.A., Cantwell, S.L., 1999. The effect of opioid and acepromazine premedication on the anesthetic induction dose of propofol in cats. Can. Vet. J. 40, 867–870.

Hao, X., Ou, M., Zhang, D., Zhao, W., Yang, Y., Liu, J., Yang, H., Zhu, T., Li, Y., Zhou, C., 2020. The effects of general anesthetics on synaptic transmission. Curr. Neuropharmacol. 18, 936–965. https://doi.org/10.2174/1570159×18666200227125854.

Hubel, D.H., Wiesel, T.N., 1962. Receptive fields, binocular interaction and functional architecture in the cat's visual cortex. J. Physiol. 160, 106–154. https://doi.org/10.1113/jphysiol.1962.sp006837.

Hübener, M., Shoham, D., Grinvald, A., Bonhoeffer, T., 1997. Spatial relationships among three columnar systems in cat area 17. J. Neurosci. 17, 9270–9284. https://doi.org/10.1523/JNEUROSCI.17-23-09270.1997.

Hudetz, A.G., Liu, X., Pillayet, S., 2015. Dynamic repertoire of intrinsic brain states is reduced in propofol-induced unconsciousness. Brain Connect 5, 10–22. https://doi.org/10.1089/brain.2014.0230.

Inoue, Y., Shibuya, I., Kabashima, N., Noguchi, J., Harayama, N., Ueta, Y., Sata, T., Shigematsu, A., Yamashita, H., 1999. The mechanism of inhibitory actions of propofol on rat supraoptic neurons. Anesthesiology 91, 167–178. https://doi.org/10.1097/00000542-199907000-00025.

Ishizawa, Y., Ahmed, O.J., Patel, S.R., Gale, J.T., Sierra-Mercado, D., Brown, E.N., Eskandar, E.N., 2016. Dynamics of propofol-induced loss of consciousness across primate neocortex. J. Neurosci. 36, 7718–7726. https://doi.org/10.1523/JNEUROSCI.4577-15.2016.

Issa, N.P., Trepel, C., Stryker, M.P., 2000. Spatial frequency maps in cat visual cortex. J. Neurosci. 20, 8504–8514. https://doi.org/10.1523/JNEUROSCI.20-22-08504.2000.

Jensen, C.S., Rasmussen, H.B., Misonou, H., 2011. Neuronal trafficking of voltage-gated potassium channels. Mol. Cell. Neurosci. 48, 288–297. https://doi.org/10.1016/j.mcn.2011.05.007.

Kalatsky, V.A., 2009. Fourier approach for functional imaging. In: Frostig, R.D. (Ed.), Vivo Optical Imaging of Brain Function, second ed.,. CRC Press/Taylor & Francis, Boca Raton Florida, p. 10 (Chapter).

Kalatsky, V.A., Stryker, M.P., 2003. New paradigm for optical imaging: temporally encoded maps of intrinsic signal. Neuron 38, 529–545. https://doi.org/10.1016/s0896-6273(03)00286-1.

Kaneko, K., Koyanagi, Y., Oi, Y., Kobayashi, M., 2016. Propofol-induced spike firing suppression is more pronounced in pyramidal neurons than in fast-spiking neurons in the rat insular cortex. Neuroscience 339, 548–560. https://doi.org/10.1016/j.neuroscience.2016.10.016.

Kaschube, M., Schnabel, M., Löwel, S., Coppola, D.M., White, L.E., Wolf, F., 2010. Universality in the evolution of orientation columns in the visual cortex. Science 330, 1113–1116. https://doi.org/10.1126/science.1194869.

Kay, N.H., Uppington, J., Sear, J.W., Allen, M.C., 1985. Use of an emulsion of ICI 35868 (propofol) for the induction and maintenance of anaesthesia. Br. J. Anaesth. 57, 736–742. https://doi.org/10.1093/bja/57.8.736.

Kenet, T., Bibitchkov, D., Tsodyks, M., Grinvald, A., Arieli, A., 2003. Spontaneously emerging cortical representations of visual attributes. Nature 425, 954–956. https://doi.org/10.1038/nature02078.

Kennedy, H., Orban, G.A., 1979. Preferences for horizontal or vertical orientation in cat visual cortical neurons. J. Physiol. 269, 61P–62P.

Kobayashi, M., Oi, Y., 2017. Actions of propofol on neurons in the cerebral cortex. J. Nippon Med. Sch. 84, 165–169. https://doi.org/10.1272/jnms.84.165.

Langley, M.S., Heel, R.C., 1988. Propofol. A review of its pharmacodynamic and pharmacokinetic properties and use as an intravenous anaesthetic. Drugs 35, 334–372. https://doi.org/10.2165/00003495-198835040-00002.

Leventhal, A.G., Hirsch, H.V.B., 1977. Effects of early experience upon orientation sensitivity and binocularity of neurons in visual cortex of cats. Proc. Natl. Acad. Sci. U. S. A. 74, 1272–1276. https://doi.org/10.1073/pnas.74.3.1272.

Li, B., Peterson, M.R., Freeman, R.D., 2003. Oblique effect: A neural basis in the visual cortex. J. Neurophysiol. 90, 204–217. https://doi.org/10.1152/jn.00954.2002.

Li, W., Wait, S.D., Ogg, R.J., Scoggins, M.A., Zou, P., Wheless, J., Boop, F.A., 2013. Functional magnetic resonance imaging of the visual cortex performed in children under sedation to assist in presurgical planning. J. Neurosurg. Pediatr. 11, 543–546. https://doi.org/10.3171/2013.1.PEDS12401.

Liang, Z., Shen, W., Shou, T., 2007. Enhancement of oblique effect in the cat's primary visual cortex via orientation preference shifting induced by excitatory feedback from higher-order cortical area 21a. Neuroscience 145, 377–383. https://doi.org/10.1016/j.neuroscience.2006.11.051.

Lingamaneni, R., Birch, M.L., Hemmings, H.C.Jr, 2001. Widespread inhibition of sodium channel-dependent glutamate release from isolated nerve terminals by isoflurane and propofol. Anesthesiology 95, 1460–1466. https://doi.org/10.1097/00000542-200112000-00027.

Liu, Q.Z., Hao, M., Zhou, Z.Y., Ge, J.L., Wu, Y.C., Zhao, L.L., Wu, X., Feng, Y., Gao, H., Li, S., Xue, L., 2019. Propofol reduces synaptic strength by inhibiting sodium and calcium channels at nerve terminals. Protein Cell 10, 688–693. https://doi.org/10.1007/s13238-019-0624-1.

Liu, X., Pillay, S., Li, R., Vizuete, J.A., Pechman, K.R., Schmainda, K.M., Hudetz, A.G., 2013. Multiphasic modification of intrinsic functional connectivity of the rat brain during increasing levels of propofol. Neuroimage 83, 581–592. https://doi.org/10.1016/j.neuroimage.2013.07.003.

Logginidou, H.G., Li, B.H., Li, D.P., Lohmann, J.S., Schuler, H.G., DiVittore, N.A., Kreiser, S., Cronin, A.J., 2003. Propofol suppresses the cortical somatosensory evoked potential in rats. Anesth. Analg. 97, 1784–1788. https://doi.org/10.1213/01.ANE.0000090318.16879.A8.

Löwel, S., Freeman, B., Singer, W., 1987. Topographic organization of the orientation column system in large flat-mounts of the cat visual cortex: a 2-deoxyglucose study. J. Comp. Neurol. 255, 401–415. https://doi.org/10.1002/cne.902550307.

Major, E., Verniquet, A.J., Waddell, T.K., Savege, T.M., Hoffler, D.E., Aveling, W., 1981. A study of three doses of ici 35 868 for induction and maintenance of anaesthesia. Br. J. Anaesth. 53, 267–272. https://doi.org/10.1093/bja/53.3.267.

Marik, P.E., 2004. Propofol: therapeutic indications and side-effects. Curr. Pharm. Des. 10, 3639–3649. https://doi.org/10.2174/1381612043382846.

Martella, G., De Persis, C., Bonsi, P., Natoli, S., Cuomo, D., Bernardi, G., Calabresi, P., Pisani, A., 2005. Inhibition of persistent sodium current fraction and voltage-gated L-type calcium current by propofol in cortical neurons: implications for its antiepileptic activity. Epilepsia 46, 624–635. https://doi.org/10.1111/j.1528-1167.2005.34904.x.

Mayhew, J.E., Askew, S., Zheng, Y., Porrill, J., Westby, G.W., Redgrave, P., Rector, D.M., Harper, R., 1996. Cerebral vasomotion: a 0.1 Hz oscillation in reflected light imaging of neural activity. NeuroImage 4, 183–193. https://doi.org/10.1006/nimg.1996.0069.

Meng, J., Li, Z., Li, H., Zhu, J., Yu, H., 2018. The common and distinct orientation adaptation effect at pinwheel centers in areas 21a and 17 of cats. Neuroscience 379, 77–92. https://doi.org/10.1016/j.neuroscience.2018.03.005.

Monteiro, E.R., Nunes-Junior, J.S., Bressan, T.F., 2014. Randomized clinical trial of the effects of a combination of acepromazine with morphine and midazolam on sedation, cardiovascular variables and the propofol dose requirements for induction of anesthesia in dogs. Vet. J. 200, 157–161. https://doi.org/10.1016/j.tvjl.2014.01.018.

Morgan, D.W., Legge, K., 1989. Clinical evaluation of propofol as an intravenous anaesthetic agent in cats and dogs. Vet. Rec. 124, 31–33. https://doi.org/10.1136/vr.124.2.31.

Movshon, J.A., Thompson, I.D., Tolhurst, D.J., 1978. Spatial and temporal contrast sensitivity of neurones in areas 17 and 18 of the cat's visual cortex. J. Physiol. 283, 101–120. https://doi.org/10.1113/jphysiol.1978.sp012490.

Müller, T., Stetter, M., Hübener, M., Sengpiel, F., Bonhoeffer, T., Gödecke, I., Chapman, B., Löwel, S., Obermayer, K., 2000. An analysis of orientation and ocular dominance patterns in the visual cortex of cats and ferrets. Neural Comput 12, 2573–2595. https://doi.org/10.1162/089976600300014854.

Ohki, K., Matsuda, Y., Ajima, A., Kim, D.S., Tanaka, S., 2000. Arrangement of orientation pinwheel centers around area 17/18 transition zone in cat visual cortex. Cereb. Cortex 10, 593–601. https://doi.org/10.1093/cercor/10.6.593.

Orban, G.A., Kennedy, H., 1981. The influence of eccentricity on receptive field types and orientation selectivity in areas 17 and 18 of the cat. Brain Res 208, 203–208. https://doi.org/10.1016/0006-8993(81)90633-8.

Ota, T., Kawai, K., Kamada, K., Kin, T., Saito, N., 2010. Intraoperative monitoring of cortically recorded visual response for posterior visual pathway. J. Neurosurg. 112, 285–294. https://doi.org/10.3171/2009.6.JNS081272.

Ouyang, W., Wang, G., Hemmings Jr., H.C., 2003. Isoflurane and propofol inhibit voltage-gated sodium channels in isolated rat neurohypophysial nerve terminals. Mol. Pharmacol. 64, 373–381. https://doi.org/10.1124/mol.64.2.373.

Pascoe, P.J., Ilkiw, J.E., Frischmeyer, K.J., 2006. The effect of the duration of propofol administration on recovery from anesthesia in cats. Vet. Anaesth. Analg. 33, 2–7. https://doi.org/10.1111/j.1467-2995.2005.00216.x.

Payne, B.R., 1990. Function of the corpus callosum in the representation of the visual field in cat visual cortex. Vis. Neurosci. 5, 205–211. https://doi.org/10.1017/s0952523800000225.

Priebe, N.J., 2016. Mechanisms of orientation selectivity in the primary visual cortex. Annu. Rev. Vis. Sci. 2, 85–107. https://doi.org/10.1146/annurev-vision-111815-114456.

Raszplewicz, J., MacFarlane, P., West, E., 2013. Comparison of sedation scores and propofol induction doses in dogs after intramuscular premedication with butorphanol and either dexmedetomidine or medetomidine. Vet. Anaesth. Analg. 40, 584–589 https://10.1111/vaa.12072.

Ratnakumari, L., Hemmings, H.C.Jr, 1997. Effects of propofol on sodium channel-dependent sodium influx and glutamate release in rat cerebrocortical synaptosomes. Anesthesiology 86, 428–439. https://doi.org/10.1097/00000542-199702000-00018.

Ratzlaff, E.H., Grinvald, A., 1991. A tandem-lens epifluorescence macroscope: hundred-fold brightness advantage for wide-field imaging. J. Neurosci. Meth 36, 127–137. https://doi.org/10.1016/0165-0270(91)90038-2.

Reed, S.J., Plourde, G., 2015. Attenuation of high-frequency (50-200 Hz) thalamocortical EEG rhythms by propofol in rats is more pronounced for the thalamus than for the cortex. PLoS One 10, e0123287. https://doi.org/10.1371/journal.pone.0123287.

Rehberg, B., Duch, D.S., 1999. Suppression of central nervous system sodium channels by propofol. Anesthesiology 91, 512–520. https://doi.org/10.1097/00000542-199908000-00026.

Reilly, C., Nimmo, W., 1987. New intravenous anaesthetics and neuromuscular blocking drugs. A review of their properties and clinical use. Drugs 34, 115–119. https://doi.org/10.2165/00003495-198734010-00004.

Ribot, J., Tanaka, S., O'Hashi, K., Ajima, A., 2008. Anisotropy in the representation of direction preferences in cat area 18. Eur. J. Neurosci. 27, 2773–2780. https://doi.org/10.1111/j.1460-9568.2008.06219.x.

Ribot, J., Aushana, Y., Bui-Quoc, E., Milleret, C., 2013. Organization and origin of spatial frequency maps in cat visual cortex. J. Neurosci. 33, 13326–13343. https://doi.org/10.1523/JNEUROSCI.4040-12.2013.

Rochefort, N.L., Buzás, P., Kisvárday, Z.F., Eysel, U.T., Milleret, C., 2007. Layout of transcallosal activity in cat visual cortex revealed by optical imaging. Neuroimage 36, 804–821. https://doi.org/10.1016/j.neuroimage.2007.03.006.

Rose, D., Blakemore, C., 1974. Effects of bicuculline on functions of inhibition in visual cortex. Nature 249, 375–377. https://doi.org/10.1038/249375a0.

Samonds, J.M., Bonds, A.B., 2005. Gamma oscillation maintains stimulus structure-dependent synchronization in cat visual cortex. Epub 2004 Jul 28. J. Neurophysiol. 93, 223–236. https://doi.org/10.1152/jn.00548.2004.

Sano, T., Nishimura, R., Mochizuki, M., Hara, Y., Tagawa, M., Sasaki, N., 2003. Clinical usefulness of propofol as an anesthetic induction agent in dogs and cats. J. Vet. Med. Sci. 65, 641–643. https://doi.org/10.1292/jvms.65.641.

Shen, W., Liang, Z., Shou, T., 2008. Weakened feedback abolishes neural oblique effect evoked by pseudo-natural visual stimuli in area 17 of the cat. Neurosci. Lett. 437, 65–70. https://doi.org/10.1016/j.neulet.2008.03.054.

Short, C.E., Bufalari, A., 1999. Propofol anesthesia. Vet. Clin. North Am. Small Anim. Pract. 29, 747–778. https://doi.org/10.1016/s0195-5616(99)50059-4.

Shumikhina, S.I., Bondar, I.V., Svinov, M.M., 2018. Dynamics of stability of orientation maps recorded with optical imaging. Neuroscience 374, 49–60. https://doi.org/10.1016/j.neuroscience.2018.01.030.

Song, C.Y., Xi, H.J., Yang, L., Qu, L.H., Yue, Z.Y., Zhou, J., Cui, X.G., Gao, W., Wang, N., Pan, Z.W., Li, W.Z., 2011. Propofol inhibited the delayed rectifier potassium current Ik via activation of protein kinase C epsilon in rat parietal cortical neurons. Eur. J. Pharmacol. 653, 16–20. https://doi.org/10.1016/j.ejphar.2010.10.072.

Stone, J., Fukuda, Y., 1974. The naso-temporal division of the cat's retina re-examined in terms of W-, X- and Y-cells. J. Comp. Neur. 155, 377–394. https://doi.org/10.1002/cne.901550402.

Taboada, F.M., Murison, P.J., 2010. Induction of anaesthesia with alfaxalone or propofol before isoflurane maintenance in cats. Vet. Rec. 167, 85–89. https://doi.org/10.1136/vr.b4872.

Tan, P.P., Shyr, M.H., Yang, C.H., Kuo, T.B., Pan, W.H., Chan, S.H., 1993. Power spectral analysis of the electroencephalographic and hemodynamic correlates of propofol anesthesia in the rat: intravenous infusion. Neurosci. Lett. 160, 205–208. https://doi.org/10.1016/0304-3940(93)90414-g.

Taylor, P.M., Chengelis, C.P., Miller, W.R., Parker, G.A., Gleason, T.R., Cozzi, E., 2012. Evaluation of propofol containing 2% benzyl alcohol preservative in cats. Contr. Clin. Trial. J. Feline Med. Sur. 14, 516–526. https://doi.org/10.1177/1098612×12440354.

Toth, L.J., Rao, S.C., Kim, D.S., Somers, D., Sur, M., 1996. Subthreshold facilitation and suppression in primary visual cortex revealed by intrinsic signal imaging. Proc. Natl. Acad. Sci. USA 93, 9869–9874. https://doi.org/10.1073/pnas.93.18.9869.

Ts'o, D.Y., Frostig, R.D., Lieke, E.E., Grinvald, A., 1990. Functional organization of primate visual cortex revealed by high resolution optical imaging. Science 249, 417–420. https://doi.org/10.1126/science.2165630.

Vanzetta, I., Grinvald, A., 1999. Increased cortical oxidative metabolism due to sensory stimulation: implications for functional brain imaging. Science 286, 1555–1558. https://doi.org/10.1126/science.286.5444.1555.

Vidyasagar, T.R., Eysel, U.T., 2015. Origins of feature selectivities and maps in the mammalian primary visual cortex. Trends Neurosci. 38, 475–485. https://doi.org/10.1016/j.tins.2015.06.003.

Vidyasagar, T.R., Pei, X., Volgushev, M., 1996. 1996. Multiple mechanisms underlying the orientation selectivity of visual cortical neurons. Trends Neurosci. 19, 272–277. https://doi.org/10.1016/S0166-2236(96)20027-X.

Wang, G., 2004. Functional segregation of plural regions representing cardinal contours in cat primary visual cortex. Eur. J. Neurosci. 20, 1906–1914. https://doi.org/10.1111/j.1460-9568.2004.03626.x.

Wang, G., Ding, S., Yunokuchi, K., 2003a. Difference in the representation of cardinal and oblique contours in cat visual cortex. Neurosci. Lett. 338, 77–81. PMID: 12565144.

Wang, G., Ding, S., Yunokuchi, K., 2003b. Representation of cardinal contour overlaps less with representation of nearby angles in cat visual cortex. J. Neurophysiol. 90, 3912–3920. https://doi.org/10.1152/jn.00219.2003.

Weaver, B.M., Raptopoulos, D., 1990. Induction of anaesthesia in dogs and cats with propofol. Vet. Rec. 126, 617–620.

Ying, S.W., Abbas, S.Y., Harrison, N.L., Goldstein, P.A., 2006. Propofol block of Ih contributes to the suppression of neuronal excitability and rhythmic burst firing in thalamocortical neurons. Eur. J. Neurosci. 23, 465–480. https://doi.org/10.1111/j.1460-9568.2005.04587.x.

Yu, H.B., Shou, T.D., 2000. The oblique effect revealed by optical imaging in primary visual cortex of cats. Acta Physiol. Sin. 52, 431–434 (Chinese).

Zepeda, A., Arias, C., Sengpiel, F., 2004. Optical imaging of intrinsic signals: recent developments in the methodology and its applications. J. Neurosci. Methods 136, 1–21. https://doi.org/10.1016/j.jneumeth.2004.02.025.

Zhang, Y.Z., Zhang, R., Zeng, X.Z., Song, C.Y., 2016. The inhibitory effect of propofol on Kv2.1 potassium channel in rat parietal cortical neurons. Neurosci. Lett. 616, 93–97. https://doi.org/10.1016/j.neulet.2016.01.058.

Zhao, F., Jin, T., Wang, P., Kim, S.-G., 2007. Isoflurane anesthesia effect in functional imaging studies. NeuroImage 38, 3–4. https://doi.org/10.1016/j.neuroimage.2007.06.040.